deposit pattern was circular for the impactors with circular jets, the point at which the jet centerline intersected the impaction substrate should be the same at the center of the particle deposit with a circular shape. Using the image analysis software, X and Y values were automatically calculated for each deposited particle based on their horizontal and vertical locations on the image captured by the OPM. Since the particle depositions were symmetric, i.e., circular, we defined the means of all the particle locations, i.e., means of X and Y values of all the particles, as a center of the particle depositions. To reduce the influence of the particles located at outlier points on estimation of the center of the particle deposition, the geometric means, instead of the arithmetic means, were used. The geometric means were calculated separately for X and Y coordinates using each X and Y value of the deposited particles, and the mean X and Y individually calculated were combined to define a point as a central point of the particle deposition (Figure 4.2). The distances of each particle from the central point of the deposition were determined based on the pair of X and Y values calculated in this manner.

The particle deposit densities per unit area (numbers mm^{-2}) were examined along the distance from the central point of the particle deposition (Figure 4.5). The result indicated the particles were densely deposited around the center of the deposition on the greased impaction substrates while they were dispersedly distributed on the non-greased substrates. Furthermore, the particle deposit densities on the greased and non-greased impaction substrates were inverted approximately around 2.6 mm of the distance, suggesting some particles were once impacted on the inner part of the deposition and hereafter relocated to the outer part. Furthermore, the particle numbers in each concentric annulus with constant radius intervals (= 0.2175 mm) from the center

of the depositions are shown in Figure 4.6. As noted above, the differences observed within each distance interval could not provide the fractions of instantaneous particle losses on these areas because the location of particles represented the final landing points, and not necessary the first impaction points.

The particle deposition patterns on the impaction substrates were investigated for size-fractionated particles (Figure 4.7). The particles were classified into 6 size categories, i.e., d_{PA} of <10, 10-15, 15-20, 20-25, 25-30 and >30 μm. Figure 4.7 suggests large amounts of the small particles especially with d_{PA} <10 μm were captured in areas distant from the jet centerline, while the large particles especially with d_{PA} >20 μm were not even recaptured on the stage. Thus, overall dispersion of the particles on the non-greased impaction substrate was due to bounces and/or reentrainments of the smaller particles. Meanwhile, the larger particles were found to be completely lost from the stage.

4.4.2. Sensitivity of the time-integrated methods

In the experiments using the greased and non-greased impaction substrates, 7.5 μg of the particles were collected on the greased substrates while 2.7 μg of them were on the non-greased substrates at 54 % RH assuming the spherical particles having unit density (= 1000 kg m^{-3}). In the case of 84 % RH, 6.7 μg of the particles were collected on the greased substrates while 3.5 μg were on the non-greased substrates. Since a practical limit of sensitivity for weighing most air-sampling filters by microbalances is 10 μg in general (Hinds, 1999), it is apparent that the microscopic method is sensitive to analyze the particle size distributions well below the detection limits of microbalances.

To verify the detection sensitivity of the microscopic methods, the time-course

accumulations of the particles on a filter were investigated by both of microscopic and direct-weighing methods. The microscopic images of the particles collected on the blank and 15- and 180-min sampling filters are shown in Figure 4.8. The time-course accumulation of the particles was evident based on the microscopic images. In Figure 4.9, numbers of particles with diameters larger than 10 μm observed by the OPM as well as masses of the particles weighed by the analytical balance were plotted in time series. The figure illustrates the OPM could detect the time-course accumulation of the particles on the filter while the analytical balance was incapable of detecting the difference.

In Figure 4.10, the particle deposit densities are shown with the area subjected to the microscopic observation. As shown in the figure, the calculated particle deposit densities become stable with increase of the surface area of the filter subjected to the microscopic observation. While the results in Figure 4.9 were obtained based on the microscopic observation of the 50-mm^2 filter surface, calculated particle numbers per unit area of the filter surface are sufficiently stable by observing the 50-mm^2 filter surface (Figure 4.10).

Meanwhile, Figure 4.11 illustrates frequencies of the particles numbers observed on the filter surfaces having an area of 1 mm^2. The theoretical distribution based on the Poisson distribution with an expected value of 13.1, i.e., the mean of the particle numbers on the 1-mm^2 filter surfaces (n = 150), is shown in the figure, too. The experimental distribution conforms to the theoretical Poisson distribution, indicating the particles are randomly distributed on the filter surface. The standard error (SE) in counting randomly distributed particles are calculated as follows:

$$\mathrm{SE} = 1/\sqrt{N}\,, \tag{4.1}$$

where N is the number of observed particles. Using this equation, variability of the counted data can be defined. In Figure 4.12, the calculated SE of the particle numbers per unit area of the filter with increase of the area subjected to the microscopic observation is shown. The figure demonstrates the calculated SE becomes lower with increase of the area subjected to the microscopic observation. For instance, SE of 3.9 % was calculated by observing the 50-mm^2 filter surface. Nevertheless, it should be stated the values of SE were not dependent on the areas subjected to the microscopic observation but on the numbers of the observed particles. Therefore, if the number of the particles deposited per unit area is smaller, the value of SE becomes larger even though the area subjected to the microscopic observation is the same. The variability in counting randomly distributed particles is generally equivalent as that defined for counting the number of asbestos fibers on a membrane filter described by the National Institute for Occupational Safety and Health for instance (NIOSH, 1994).

4.5. Summary

A line-sensing optical microscope (OPM) was used to investigate an entire area of a particle deposition generated by an individual acceleration air nozzle in a high volume Andersen sampler. Using its advantage of broad range microscopic observations accomplished by a line-sensing mechanism, the spatial distributions of the particles deposited on the greased and non-greased Teflon impaction surfaces were investigated. The particle size distributions as well as their spatial locations on the greased and non-greased substrates were compared to characterize the particle loss from the smooth impaction substrates. The particles deposited on the impaction substrates were automatically counted, sized and located by the image analysis software bundled

with the OPM. The result confirmed reproducible collection characteristics among each nozzle even though application of the greasing material increased the collection efficiency ($N = 245 \pm 24$ and 119 ± 18 for the greased and non-greased substrates at 54 % RH, and $N = 488 \pm 53$ and 368 ± 77 at 84 % RH, respectively) and altered the size distribution of collected particles to the larger side (15.0 and 12.6 μm of geometric mean diameters for the particles collected on the greased and non-greased impaction substrates at 54 % RH, and 12.2 and 11.2 μm at 84 % RH, respectively). In these experiments, approximately 65 % of the particle mass and 50 % of the particle number were lost from the non-greased substrates at 54 % RH while 45 % by mass and 25 % by number were underestimated at 84 % RH, assuming spherical particles with uniform density. The result indicated the errors in the particle size distribution measurements due to the particle bounces and/or reentrainments were more significant for the mass concentration measurements rather than for number concentration measurements. Moreover, the large particles were selectively lost from the non-greased impaction substrates. It was found in this study that particle loss due to the bounce and/or reentrainment occurred more significantly at lower RH.

The microscopic analyses showed the particles were densely deposited around the jet centerline on the greased impaction substrates while they were dispersedly distributed on the non-greased substrates. Moreover, it was found that particle deposit densities on the greased and non-greased impaction substrates were inverted approximately around 2.6 mm of the distance from the central point of the deposition. The particle deposition patterns were also investigated for size fractionated particle groups. The result of the spatial distributions by particle size suggests that dispersion of particle on the impaction substrate is due to bounce and/or reentrainment of smaller

particles especially with d_{PA} <10 μm.

4.6. Conclusions in the thesis

In the CI, the particle size classification is achieved by means of inertial forces of the particles. Nevertheless, the particle size classifications are often deteriorated by the particle bounce on the impaction substrates as was demonstrated in this chapter. In consequence, the trueness in particle sizing was lowered in the CI. Meanwhile, the OPM is advantageous in terms of particle sizing trueness since it directly measures the particle sizes and does not rely on indirect properties such as particle inertial forces. As was explained in Chapter 3, the particle sizing trueness of the OPM is high since it permits direct measurement of the particle size and shape. Moreover, the sensitivity of the OPM method was exemplified in this Chapter by roughly calculating the particle masses based on information of the particle number distributions characterized by the OPM. For instance, we found that 6.7 μg of the particles were collected on the greased substrates while 3.5 μg of them were on the non-greased substrates at 84 % RH assuming the spherical particles having unit density. Since a practical limit of sensitivity for weighing most air-sampling filters by microbalances is 10 μg in general (Hinds, 1999), it is apparent that the microscopic method is sensitive to analyze the particle size distributions well below the detection limits of microbalances. The sensitivity of the OPM was demonstrated by comparing that by a direct weighing method by an analytical microbalance, too. We found the OPM could detect the time-course accumulation of the particles on the filter while the analytical balance was incapable of detecting the difference. Furthermore, spatial characterization of the particles on the impactor substrates was possible using the line-sensing mechanism of

the OPM. While various studies have investigated particle bounce from the impactor substrates using various methodologies, the present study was the first to visualize entire images of the particle depositions on the impactor substrates and analyze possible phenomena of the particles on the impactor substrates. Therefore, the ability to characterize spatial distributions of the particles is another advantages of the microscopic method.

References

Chang, M., Kim, S., & Sioutas, C. (1999). Experimental studies on particle impaction and bounce: Effects of substrate design and material. *Atmospheric Environment, 33*, 2313-2322.

Cheng, Y. S., & Yeh, H. C. (1979). Particle bounce in cascade impactors. *Environmental Science and Technology, 13*, 1392-1396.

Corn, M., & Stein, F. (1965). Re-entrainment of particles from a plane surface. *American Industrial Hygiene Association Journal, 26*, 325-336.

Dahneke, B. (1971). The capture of aerosol particles by surfaces. *Journal of Colloid Interface Science, 37*, 342-353.

Dzubay, T. H., Hines, L. E., & Stevens, R. K. (1976). Particle bounce error in cascade impactors. *Atmospheric Environment, 10*, 229-234.

Ellenbecker, M. J., Leith, D., & Price, J. M. (1980). Impaction and particle bounce at high Stokes numbers. *Journal of Air Pollution Control Association, 30*, 1224-1227.

Hinds, W. C., Liu, W. V., & Froines, J. R. (1985). Particle bounce in a personal cascade impactor: A field evaluation. *American Industrial Hygiene Association Journal, 46*, 517-523.

Hinds, W. C. (1999). *Aerosol technology: Properties, behavior, and measurement of airborne particles (2nd Ed.)*, New York, Wiley.

Kaneyasu, N. (1998). Wide ranged measurement of elemental carbon in atmospheric aerosols using spot samples on the tape filter mounted in automated SPM monitors. *Journal of Japanese Society of Atmospheric Environment, 33*, 344-356.

Marple, V. A., Rubow, K. L., Turner, W., & Spengler, J.D. (1987). Low flow rate sharp cut impactors for indoor air sampling: Design and calibration. *Journal of Air Pollution Control Association, 37*, 1303-1307.

Marple, V. A., Rubow, K. L., & Hehm, S. M. (1991). A micro-orifice uniform deposit impactor (MOUDI): Description, calibration, and use. *Aerosol Science and Technology, 14*, 434-446.

National Institute for Occupational Safety and Health (1994). Method #7400 - Asbestos and Other Fibers by PCM. <http://www.cdc.gov/niosh/nmam/pdfs/7400.pdf> Accessed 28 February 2006.

Newton, G. J., Cheng, Y. S., Barr, E. B., & Yeh, H. C. (1990). Effects of collection substrates on performance and wall losses in cascade impactor. *Journal of Aerosol Science, 21*, 467-470.

Owens, J. S. (1923). Jet dust counting apparatus. *Journal of Industrial Hygiene, 4*, 522-534.

Rao, A. K., & Whitby K. T. (1978a). Non-ideal collection characteristics of inertial impactors-I. Single-stage impactors and solid particles. *Journal of Aerosol Science, 9*, 77-86.

Rao, A. K., & Whitby K. T. (1978b). Non-ideal collection characteristics of inertial impactors-II. Cascade impactors. *Journal of Aerosol Science, 9*, 87-100.

Reischl, G. P., & John, W. (1978). The collection efficiency of impaction surface, Staub. Reinhalt. Luft. 38, 55.

Stein, S. W., Turpin, B. J., Cai, X. P., Huang, C. P. F., & McMurry, P. H. (1994). Measurements of relative humidity-dependent bounce and density for atmospheric particles using the DMA-impactor technique. *Atmospheric Environment, 28*, 1739-1746.

Turner, C. J., & Hering, S. V. (1987). Greased and oiled substrate as bounce-free impaction surfaces. *Journal of Aerosol Science, 18*, 215-224.

Vasiliou, J. G., Sorensen, D., & McMurry, P. H. (1999). Sampling at controlled relative humidity with a cascade impactor. *Atmospheric Environment, 33*, 1049-1056.

Wall, S., John, W., Wang, H-C, & Goren, S. (1990). Measurements of kinetic energy loss for particles impacting surfaces. *Aerosol Science and Technology, 12*, 926-946.

Winkler, P. (1974). Relative humidity and the adhesion of atmospheric particles to the plates of impactors. *Aerosol Science, 5*, 235-240.

Table 4.1

Specifications of impactor stages of a high volume Andersen sampler, AH-600 Model

Stage number	Size range d_a (μm)	Jets/Stage	Impactor jet diameter, D_j (mm)	Nozzle velocity (m s^{-1})
1	>7.0	300	3.48	3.31
2	3.3-7.0	296	2.14	8.74
3	2.0-3.3	300	1.54	16.88
4	1.1-2.0	296	1.05	36.31

Table 4.2

Ambient sampling conditions

Sampling date and time	RH (%)	Temperature (°C)
May 14, 2002, 11:30-13:00	54	22
August 6, 2002, 7:00-7:45	84	28

Table 4.3

Numbers and size distributions of the particles collected on the greased and non-greased Teflon impaction substrates at 54 % RH

			Size distribution [a]	
			Geometric mean diameter	
Impaction substrate	Sample [b] ID	Numbers of particles, N	d_{PA} (μm)	GSD
Greased Teflon substrate	G1	269	13.8	1.7
	G2	257	15.2	1.7
	G3	216	14.6	1.6
	G4	235	15.8	1.6
	G5	223	15.8	1.7
	G6	270	15.0	1.6
	Mean	245	15.0	1.7
	SD	24		
Non-greased Teflon Substrate	NG1	117	12.7	1.6
	NG2	103	11.2	1.8
	NG3	127	12.7	1.8
	NG4	104	13.0	1.6
	NG5	152	12.5	1.6
	NG6	111	13.4	1.8
	Mean	119	12.6	1.8
	SD	18		

[a] Based on particle's projected area diameters.

[b] Each sample was taken beneath each individual nozzle jet.

Table 4.4

Numbers and size distributions of the particles collected on the greased and non-greased Teflon impaction substrates at 84 % RH

			Size distribution [a]	
			Geometric mean diameter	
Impaction substrate	Sample [b] ID	Numbers of particles, N	d_{PA} (μm)	GSD
Greased Teflon substrate	G1	471	12.0	1.6
	G2	424	13.0	1.7
	G3	466	11.8	1.7
	G4	473	12.1	1.6
	G5	516	12.2	1.7
	G6	579	12.3	1.7
	Mean	488	12.2	1.7
	SD	53		
Non-greased Teflon Substrate	NG1	510	11.2	1.6
	NG2	281	10.8	1.6
	NG3	376	11.1	1.6
	NG4	344	11.7	1.7
	NG5	329	11.1	1.6
	NG6	368	11.2	1.6
	Mean	368	11.2	1.6
	SD	77		

[a] Based on particle's projected area diameters.

[b] Each sample was taken beneath each individual nozzle jet.

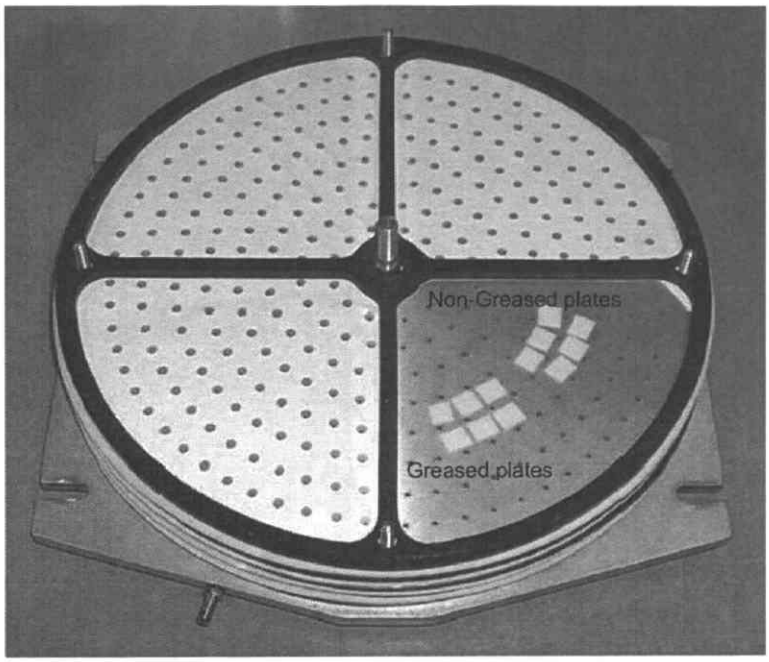

Figure 4.1. Greased and non-greased Teflon substrates on the impactor stage.

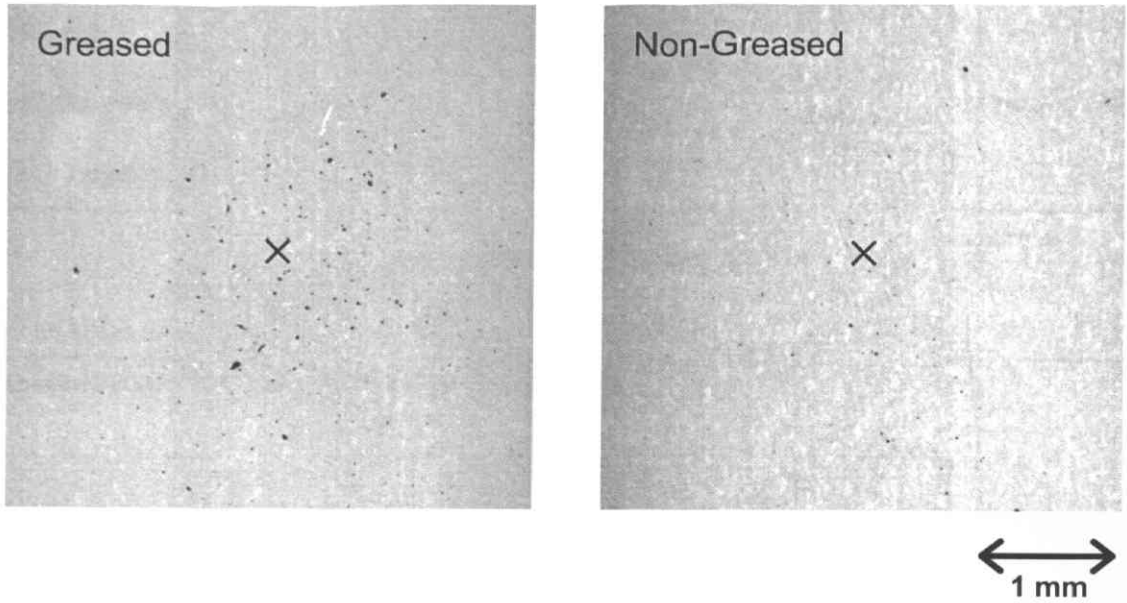

Figure 4.2. Images of particle depositions on the greased and non-greased Teflon impaction substrates with calculated centers of particle depositions.

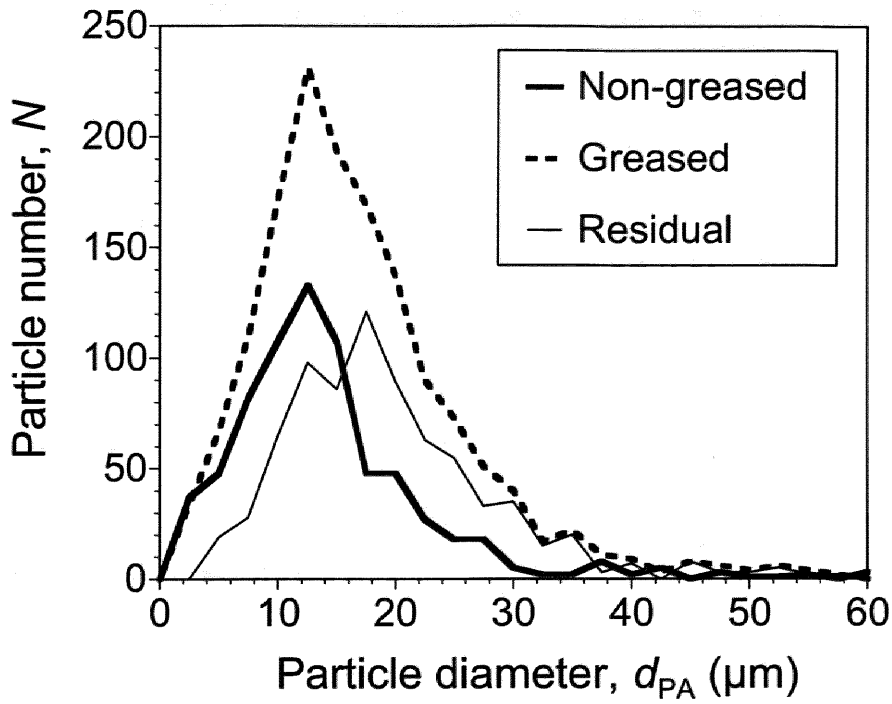

Figure 4.3. . Particle size distributions deposited on the greased and non-greased impaction substrates collected through 6 impactor nozzles at 54 % RH. Residual was calculated as differences between particle numbers on the greased and non-greased substrates.

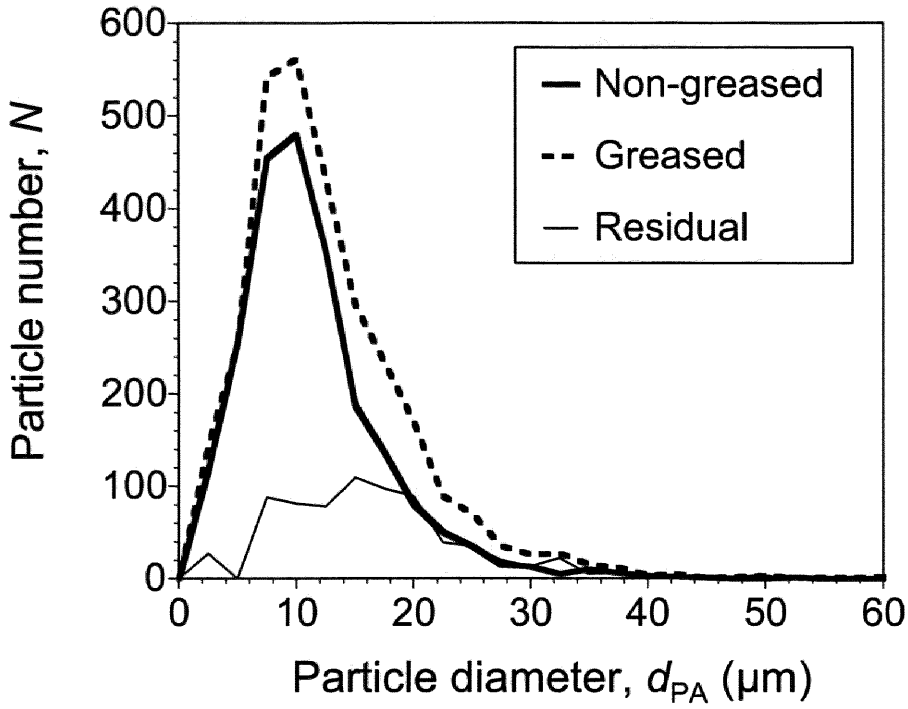

Figure 4.4. . Particle size distributions deposited on the greased and non-greased impaction substrates collected through 6 impactor nozzles at 84 % RH. Residual was calculated as differences between particle numbers on the greased and non-greased substrates.

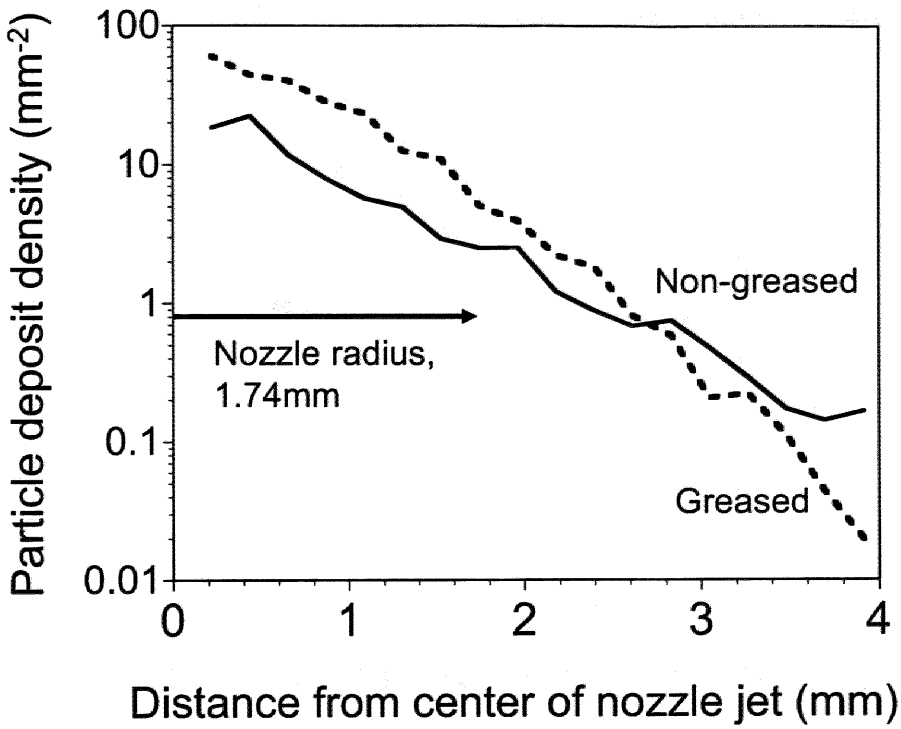

Figure 4.5. Particle deposit densities along with distances from jet centerline on the greased and non-greased Teflon impaction substrates at 54 % RH.

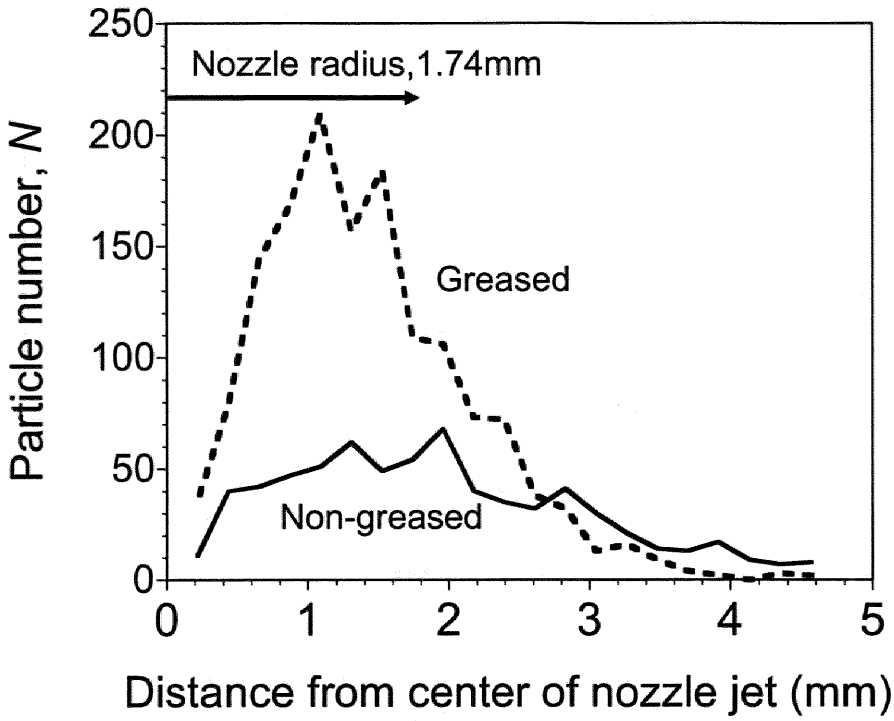

Figure 4.6. Numbers of total particles deposited on concentric annuli from the center of the nozzle jet on the greased and non-greased impaction substrates collected through 6 impactor nozzles at 54 % RH.

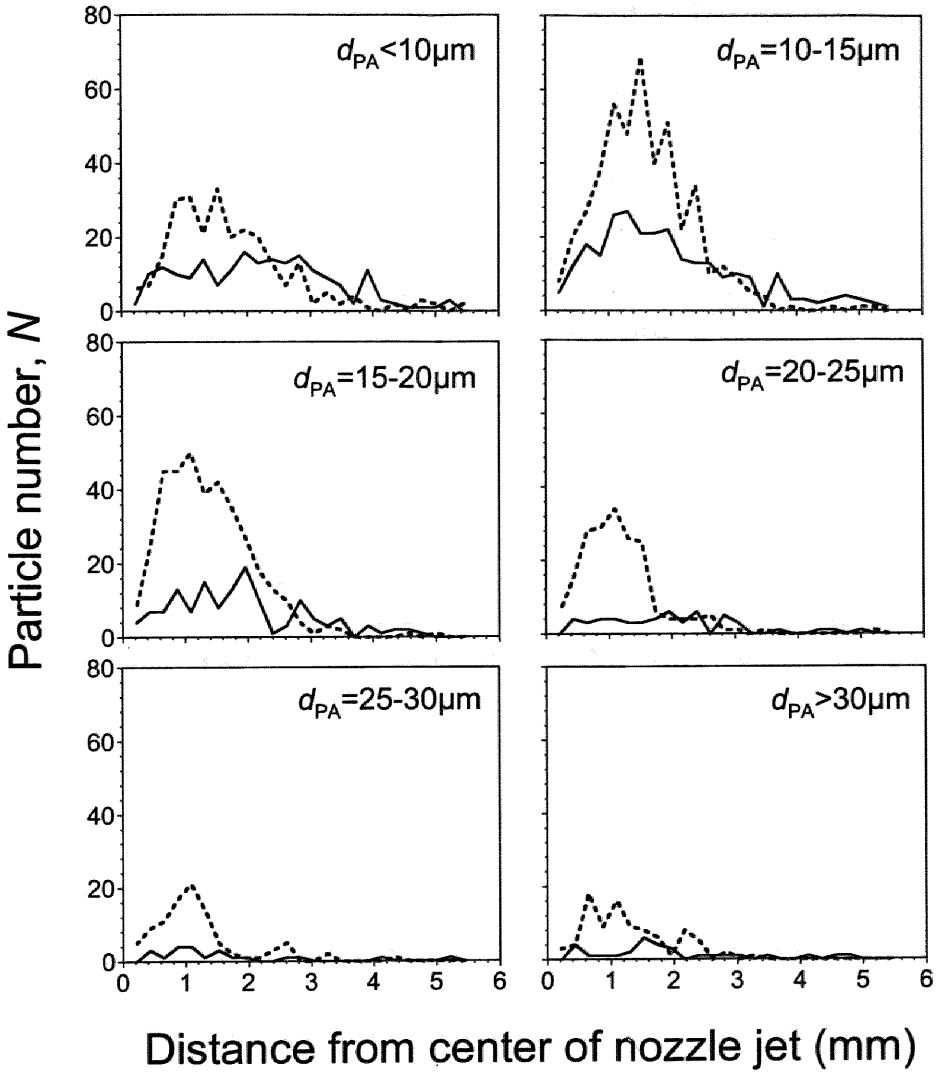

Figure 4.7. Numbers of deposited particles with d_{PA} of <10, 10-15, 15-20, 20-25, 25-30, >30 μm on concentric annuli from the center of the nozzle jet on the greased and non-greased impaction substrates collected through 6 impactor nozzles at 54 % RH.

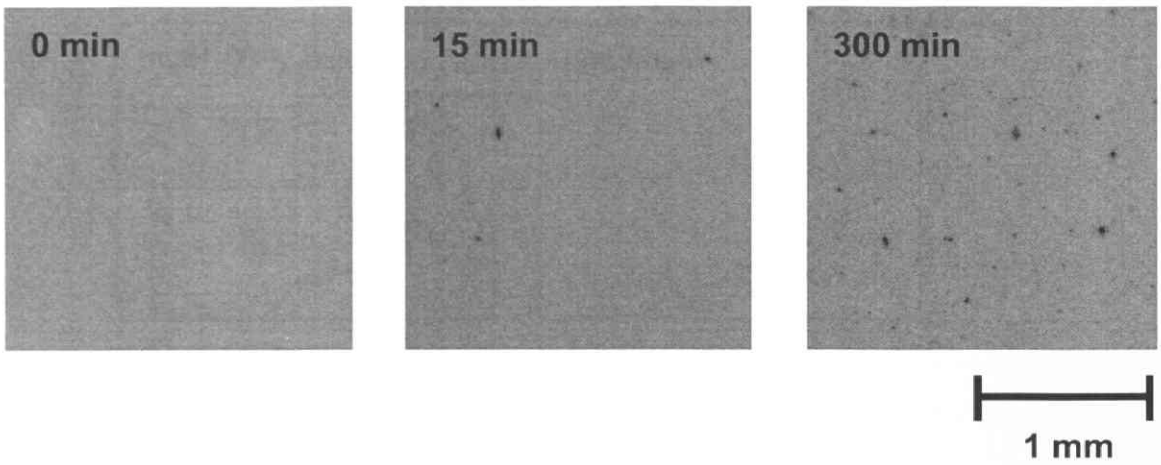

Figure 4.8. Microscopic images of the particles collected on the blank and 15- and 180-min sampling filters.

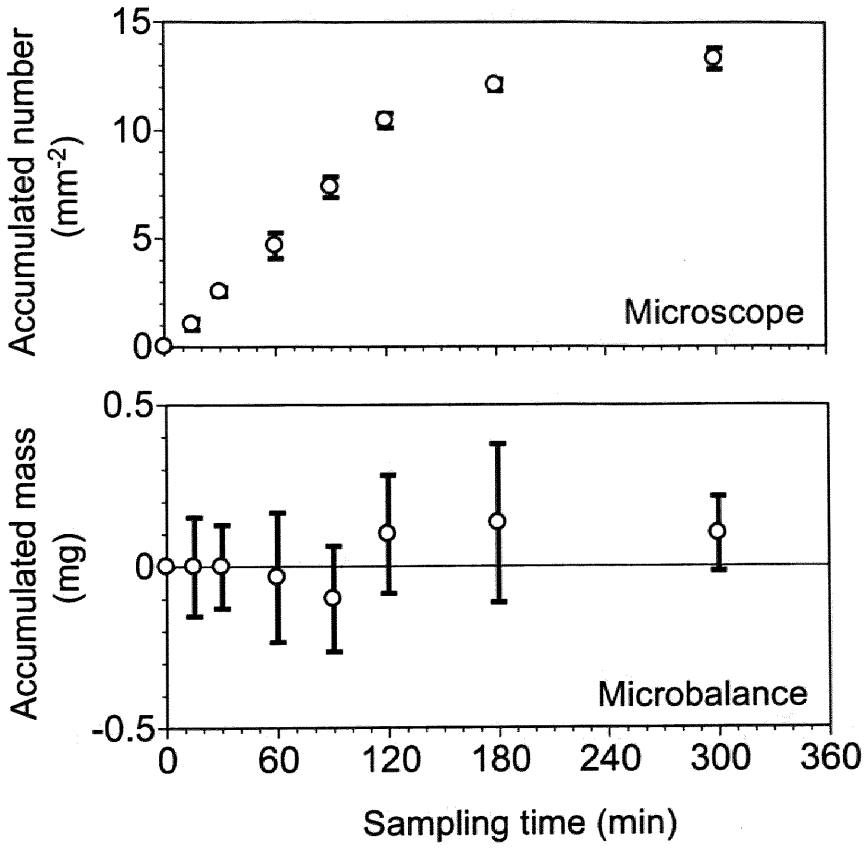

Figure 4.9. Time course of particle accumulation on the 25-mm filter by outdoor sampling with an air flow rate at 2 l min^{-1}. Error bars in the microscopic method indicate standard deviations (SD) of the particle number densities based on microscopic observations of the 50-mm^2 filter surface (n = 3). Particle masses by the microbalance are calculated by differences of the filter weights before and after the samplings (n = 3).

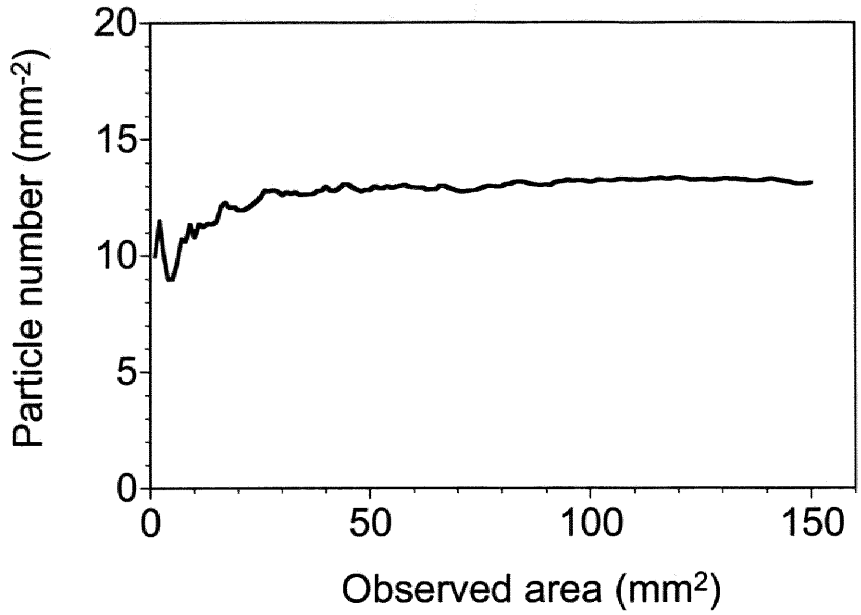

Figure 4.10. Particle deposit densities along with areas subjected to the microscopic observation.

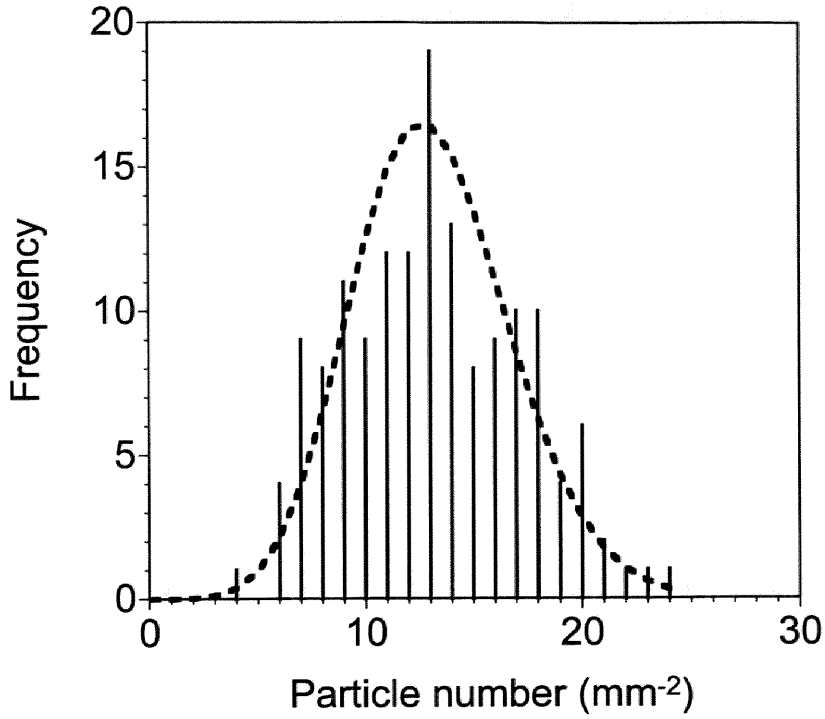

Figure 4.11. Experimental frequencies (solid bars) of the particles numbers observed on the filter surfaces having an area of 1 mm^2. Theoretical distribution (dotted line) was calculated based on the Poisson distribution with an expected value of 13.1, i.e., the mean of the particle numbers on the 1-mm^2 filter surfaces (n = 150).

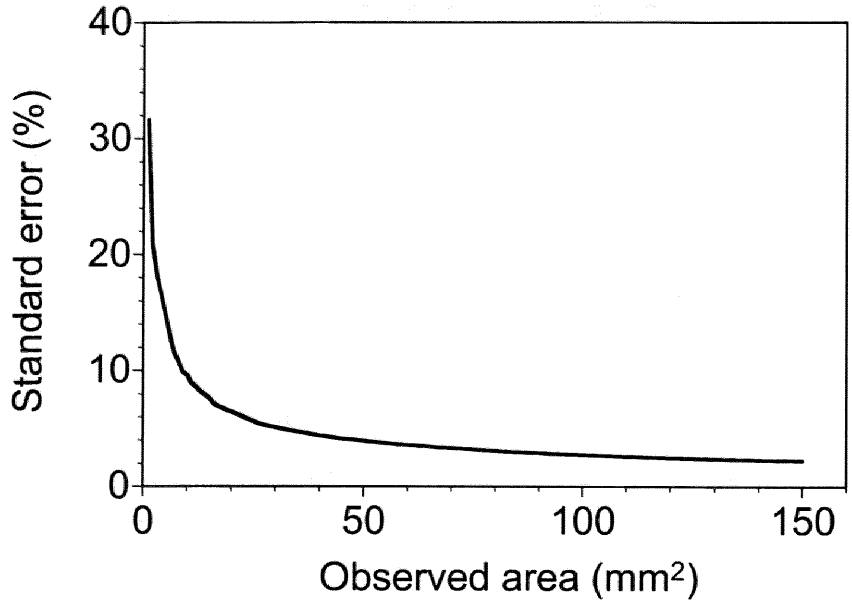

Figure 4.12. Calculated standard errors (SE) of the particle numbers per unit area of the filter with increase of the area subjected to the microscopic observation.

CHAPTER 5.
Summary of the microscopic method and its future prospects

CHAPTER 5. Summary of the microscopic method and its future prospects

5.1. Summary of the OPM

The microscopic method was found to be sensitive compared to the traditional methods such as the gravimetric analyses. In Chapter 4, the detection sensitivity of the OPM method was exemplified by roughly estimating the particle mass based on the particle number distributions characterized by the OPM. The particle mass estimated based on the particle number distributions was far below detection limits of microbalances. Furthermore, we experimentally demonstrated the OPM could detect the time-course accumulation of the particles on the filter while the analytical balance was incapable of detecting the time-course difference. Since the masses of spherical particles with diameters of 0.1, 1, 10, 100 μm having unit density (= 1000 kg m^{-3}) are calculated to be 520 ag, fg, pg and ng, respectively, the microscopic methods can detect ag order of the particles in theory while the limits of detection of microbalances are approximately 10 μg in general. Since the resolving power of the OPM is 2.7 μm, the detection limit of the OPM is equivalent to the mass of the particle having a diameter of 2.7 μm. Assuming a spherical particle having unit density, the mass of the particle is calculated to be approximately 10 pg, suggesting the detection limit of the OPM is on the order of pg if it is translated on the mass basis. Moreover, good correlations between the OPM and existing light scattering methods assured the measurement ability by the OPM method (Chapter 3). Unlike existing microscopes with stationary sample stages, it is convenient to measure a sufficient number of the particles by means of the

line-sensor camera in conjunction with the linear actuating slide of the OPM. The increase of the measured number of the particles assures the ability in the particle concentrations measurements.

Another advantage of the OPM method lies in its trueness in the particle size measurements. Since the microscopic method can directly capture the particle images, its trueness in particle sizing is generally better than those by the indirect methods, and the method often serves as a primary measurement for the calibration of other aerosol-sizing methods (Hinds, 1999). In Chapter 3, it was elucidated the particle-sizing trueness was lowered in the light scattering method since the method uses the light scattering property of the particles as an indirect measure for particle sizing. Meanwhile, the particle size classification is usually achieved by means of inertial forces of the particles in the time-integrated methods. Among these methods, the CI is the most commonly used. Nevertheless, the particle size classification characteristics are often deteriorated by the particle bounce on the impaction substrates, and trueness in particle sizing was consequently lowered in these time-integrated sampling devices (Chapter 4). In Chapter 3, the standard particles with known diameters were observed by the OPM, and the experimentally obtained particle diameters were compared with information values certified by the NIST to highlight the trueness in particle sizing by the OPM. The sizes of the standard particles characterized by the OPM were quite consistent with those of the certified values (Table 3.1).

Using the line-sensing mechanism in conjunction with the linear actuating slide of the OPM, spatial characterization of the particle depositions on the impactor substrates was possible (Chapter 4). While various studies have investigated the

bounce off of the particles from the impactor substrates, the present study was the first to visualize entire images of the particle depositions on the impactor substrates and examine the particle depositions on the impactor substrates. Therefore, the ability to characterize the spatial distributions of the particles is another advantage of the OPM method.

Overall, the characteristics of the OPM method are summarized as follows: (1) sensitivity, (2) sufficient measurement ability compared to an existing method such as a light-scattering particle counter, (3) trueness in particle sizing by directly capturing the particle images without measuring indirect properties such as light scattering, light absorption and mechanical and/or electrical mobility, (4) ability to characterize spatial distributions of the particles.

5.2. Future prospects of the OPM

The sensitivity of the microscopic method can be advantageous in various ways. In theory, increase of the sensitivity leads to decrease of required particle amount for subsequent analytical methods. Consequently, decreases of the sampling time and rate become feasible. The reduction of the sampling time provides opportunities of time-resolved particle concentration measurements while decrease of the sampling rates is ultimately attained to the passive sampling methods. Although it is generally difficult to obtain adequate amounts of the particles by the passive methods for subsequent analytical methods, the microscopic methods are expected to be sensitive to quantitate the amounts of passively collected particles.

5.2.1. Time-resolved analyses

The recent works indicate possible association between short-term excursions in particle concentrations and adverse health effects (Delfino et al., 1998; Michaels, 1998; Michaels & Kleinman, 2000). Therefore, the time-resolved analyses of airborne particulate matters are essential from the aspect of human health. Although there are several types of commercially available direct-reading aerosol monitors such as light scattering particle counters or personal nephelometers, these instruments are inappropriate to characterize chemical components of measured particles. Meanwhile, the microscopic methods are capable to analyze chemical species of the measured particles. For instance, observations by electron microscopes with a function of energy dispersive X-ray fluorescence (EDX) technique enable chemical component analysis of the measured particles. Conner & Williams (2004) used SEM with EDX to identify chemical compositions of the particles collected by personal air samplings. Moreover, the particle morphology characterized by microscopic observation is often indicative of aerosol species (e.g., Ebert et al., 2004; Liu et al., 2005). Consequently, chemical constituents can be inferred from the particle morphology.

As will be described in the subsequent section, the immunostaining methods can create opportunities to identify allergenic particles based on the stained color since the allergenic particles are selectively stained to a particular color. Although the time required to stain the allergenic particles might be of concern, the methods might be useful to measure temporal concentrations of allergenic particles because of the sensitivity of the microscopic methods. For instance, cedar pollens, causative agents of cedar pollinosis, have large intraday variations in the concentrations in air due to the effect of solar irradiation. Meanwhile, the local governments presently provide pollen

information on a daily basis. Since the patients rather need information on an hourly basis, the time-resolved measurements are strongly desirous. By using the detection sensitivity and selectivity of the microscopic methods, the time-resolved measurements of aeroallergens including cedar pollens are expected to be feasible. Using a tape filter automatically advanced every set time period, the time-resolved measurements of airborne particles are capable by repeating the measurement cycle of (1) particle sampling, (2) microscopic observation in conjunction with abovementioned chemical and/or biological constituent identification techniques, (3) digital analyses of microscopic images, (4) concentration calculations, and (4) filter exchange.

5.2.2. Passive sampling methods

The passive samplers are devices to collect airborne substances by naturally occurred mass transfers. The passive samplers are particularly convenient for personal air samplings since they are quiet, light, and easy to handle. Therefore, they have been widely used in a variety of field investigations (e.g., Yanagisawa & Nishimura, 1982; Shields & Weschler, 1987; Levy et al., 1998; Shinohara et al., 2004). While the passive sampling methods have been established for gaseous pollutants such as nitrogen oxides (NOx) or volatile organic compounds (VOCs), the methodologies are still under development for airborne particulate matters. This is primarily due to complexity in converting the particle amounts passively collected to the concentrations in air. In the passive sampling method, calculations of the particle uptake rates are essential to convert the collected amounts to the concentrations in air. Since the ambient particles are generally heterogeneous in terms of size, shape and density, contributions of each particle transport mechanism including the Brownian diffusion, gravitational settling,

inertial and electrostatic forces, are considerably varied for each particle. Consequently, unique values of the mass transfer coefficients can be hardly assumed for ambient airborne particles with heterogeneous physical characteristics.

Nevertheless, various types of passive samplers for airborne particles have been challenged in the past. For instance, a method using an electret-based material to collect airborne particles (Brown et al., 1994a, 1994b, 1995; Thorpe et al., 1999), a statistical model to estimate the particle concentrations in air based on the particle amounts passively collected on a sticky substrate (Vinzents, 1996), and a microscopic method to characterize numbers and sizes of passively collected particles (Wagner & Leith, 2001a, 2001b, 2001c) have been reported. As described above, a theoretical difficulty to convert the collected amounts to the concentrations in air lies in lack of information on particle motions in air. Since the particle motions in air are dominated by their physical properties such as size, shape and density, microscopic observations of the collected particles are essential to estimate their atmospheric behaviors. Whereas the density and dynamic shape factor, required variables for theoretical calculations, remain to be unknown even with microscopic observations, the microscopic methods are still useful for a variety of environments. For instance, adequate assumptions can be made for these unknown variables under occupational environments having known sources of relatively homogeneous aerosol particles (Wagner & Leith, 2001c).

For biological particles including aeroallergens, the settling plates are frequently used to passively collect these particles. The plates often contain appropriate nutrient media to culture the collected viable microorganisms and enumerate the grown colonies. Since the settling plate methods are simple and easy to handle, they have been widely used to assess microbial contaminations in air (e.g., Alder & Gillespie, 1964; Fitt &

Bainbridge, 1983; Lindow et al., 1988). The settling plates are also used to collect non-viable biological particles. For instance, the Durham gravity pollen collector (Durham, 1946), a kind of the settling plates, is commonly used to collect pollens on glass slides by gravitational settling. The Durham sampler consisting of a horizontally placed glass slide coated with greasing materials is normally used to evaluate the amount of airborne cedar pollens causing cedar pollinosis, an important allergic rhinoconjunctivitis in Japan (e.g., Ozasa et al., 2001). Cedar pollens collected on the greased glass slide are stained by gentian violet and enumerated by microscopic observation. It should be stated these passive samplers are generally large since they are designed as stationary samplers. Therefore, it is obvious these samplers cannot be used as personal samplers to assess personal exposures to aeroallergens.

References

Alder, V. G., & Gillespie, W. A. (1964). Pressure sores and staphylococcal cross-infection: detection of sources by means of settle-plates. *Lancet, 284*, 1356-1358.

Brown, R. C., Hemingway, M. A., Wake, D., & Thompson, J. (1995). Field trials of an electret-based passive dust sampler in metal-processing industries. *Annals of Occupational Hygiene, 39*, 603-622.

Brown, R. C., Wake, D., Thorpe, A., Hemingway, M. A., & Roff, M. (1994a). Theory and measurement of the capture of charged dust particles by electrets. *Journal of Aerosol Science, 25*, 149-163

Brown, R. C., Wake, D., Thorpe, A., Hemingway, M. A., & Roff, M. (1994b). Preliminary assessment of a device for passive sampling of airborne particulate. *Annals of Occupational Hygiene, 38*, 303-318.

Conner, T. L., & Williams, R. W. (2004). Identification of possible sources of particulate matter in the personal cloud using SEM/EDX. *Atmospheric Environment, 38*, 5305-5310

Delfino, R. J., Zeiger, R. S., Seltzer, J. M., & Street, D. H. (1998). Symptoms in pediatric asthmatics and air pollution: Differences in effects by symptom severity, anti-inflammatory medication use and particulate averaging time. *Environmental Health Perspectives, 106*, 751-761.

Durham, O. C. (1946). The volumetric incidence of atmospheric allergens. IV. A proposed standard method of gravity sampling, counting, and volumetric interpolation of results. *Journal of Allergy, 17*, 79-86.

Ebert, M., Weinbruch, S., Hoffmann, P., & Ortner, H. M. (2004). The chemical composition and complex refractive index of rural and urban influenced aerosols determined by individual particle analysis. *Atmospheric Environment, 38*, 6531-6545.

Fitt, B. D. L., & Bainbridge, A. (1983). Recovery of Pseudocercosporella herpotrichoides spores from rain-splash samples. *Phytopathology, 106*, 177-82.

Hinds, W. C. (1999). *Aerosol technology: properties, behaviour, and measurement of airborne particles (2nd Ed.)*, Wiley, New York.

Levy, J. I., Lee, K., Spengler, J. D., & Yanagisawa, Y. (1998). Impact of residential nitrogen dioxide exposure on personal exposure: an international study. *Journal of the Air and Waste Management Association, 8*, 553-560.

Lindow, S. E., Knudsen, G. R., Seidler, R. J., Walter, M. V., Lambou, V. W., Amy, P. S., Schmedding, D., Prince, V., & Hern, S. (1988). Aerial dispersal and epiphytic survival of Pseudomonas syringae during a pretest for the release of genetically engineered strains into the environment. *Applied and Environmental Microbiology, 54*, 1557-1563.

Liu, X., Zhu, J., Van Espen, P., Adams, F., Xiao, R., Dong, S., & Li, Y. (2005). Single particle characterization of spring and summer aerosols in Beijing: Formation of composite sulfate of calcium and potassium. *Atmospheric Environment, 39*, 6909-6918.

Michaels, R. A. (1998). Permissible daily airborne particle mass levels encompass brief excursions to the "London Fog" range, which may contribute to daily mortality and morbidity in communities. *Applied Occupational and Environmental Hygiene, 13*, 385-394.

Michaels, R. A., & Kleinman, M. T. (2000). Incidence and apparent health significance of brief airborne particle excursions. *Aerosol Science and Technology, 32*, 93-105.

Ozasa, K., Dejima, K., & Takenaka, H. (2002). Prevalence of Japanese cedar pollinosis among schoolchildren in Japan. *International Archives of Allergy and Immunology, 128*, 165-167.

Shields, H. C., & Weschler, C. J. (1987). Analysis of ambient concentrations of organic vapors with a passive sampler. *Journal of Air Pollution Control Association, 37*, 1039-1045.

Shinohara, N., Mizukoshi, A., & Yanagisawa, Y. (2004). Identification of responsible volatile chemicals that induce hypersensitive reactions to multiple chemical sensitivity patients. *Journal of Exposure Analysis and Environmental Epidemiology, 14*, 84-91.

Thorpe, A., Hemingway, M. A., & Brown, R. C. (1999). Monitoring of urban particulate using and electret-based passive sampler. *Applied Occupational and Environmental Hygiene, 14*, 750-758.

Vinzents, P. S. (1996). A passive personal dust monitor. *Annals of Occupational Hygiene, 40*, 261-280.

Wagner, J., & Leith, D. (2001a). Passive aerosol sampler. I: Principle of operation. *Aerosol Science and Technology, 34*, 186-192.

Wagner, J., & Leith, D. (2001b). Passive aerosol sampler. II: Wind tunnel experiments. *Aerosol Science and Technology, 34*, 193-201.

Wagner, J., & Leith, D. (2001c). Field tests of a passive aerosol sampler. *Journal of Aerosol Science, 32*, 33-48.

Yanagisawa, Y., & Nishimura, H. (1982). A badge-type personal sampler for measurement of personal exposure to NO2 and NO in ambient air. *Environment International, 8*, 235-242.

CHAPTER 6.
A passive sampler for airborne coarse particles: Personal aeroallergen sampler (PAAS)

CHAPTER 6. A passive sampler for airborne coarse particles: Personal aeroallergen sampler (PAAS)

6.1. Importance of the personal samplings

The concentrations of airborne coarse particles such as resuspended house dusts, major indoor allergens, are known to increase sharply at the moment of indoor disturbance while the concentrations decrease rapidly due to gravitational sedimentation. Consequently, the concentrations of airborne coarse particles are known to be temporally and spatially varied even in the same room (Irie et al., 1981). Since individuals are likely exposed to the particles resuspended by their own activities, the stationery monitoring does not always represent the personal exposures if the monitoring is conducted far away from the points at which individuals are located (Figure 6.1). Indeed, Ferro et al. (2004) reported personal exposure levels to airborne coarse particles are known to be higher than indoor concentration levels measured by the stationery monitors. Therefore, the stationery air monitoring is likely erroneous for assessing personal exposures to airborne coarse particles, and the ideal monitoring should be taken in the vicinity of individuals.

To collect airborne particles in the vicinity of individuals, human subjects are often asked to carry the personal air samplers. Among various types of the personal samplers, there are two types in general, i.e., active and passive samplers. While the active samplers are those operated with the pumps to actively collect target substances in air at known flow rates, the passive samplers collect the airborne substances by

naturally occurred mass transfers. Between these two methods, the passive samplers are particularly convenient for the personal air samplings since they are quiet, light, and easy to handle. Meanwhile, the active samplers are occasionally impractical for the personal air samplings because of limited lifetime of battery, noise, weight and dimension of the samplers. In particular, the active samplers are almost impossible for child subjects.

The allergen exposure in childhood is now believed to be an important determinant for initial sensitization of the immune system and subsequent progression to clinical allergic diseases (Holt et al., 1999; Platts-Mills et al., 2000; Sporik & Platts-Mills, 2001; Halken, 2003). Meanwhile, children are likely exposed to aeroallergens much higher than adults since they breathe the air more proximate to a ground as an important allergen reservoir (Figure 6.2). Indeed, our preliminary experiments (Yamamoto, N., Kumagai, K., Fujii, M., Endo, O., & Yanagisawa, Y., unpublished data) showed higher concentrations of resuspended house dusts in a child-breathing zone (Figure 6.3), suggesting children are exposed to a special risk to inhale the concentrated aerosol allergens resuspended by their own activities. To elucidate the disease expression mechanisms in early life, accurate assessments of children's exposures to aeroallergens are essential.

We have recently developed the personal aeroallergen sampler (PAAS) (Figure 6.4), a passive sampler for coarse airborne particles, to conveniently measure the personal exposures to aeroallergens such as fungal spores, cedar pollens, mite fecal pellets, and so on. The PAAS was convenient for human subjects including children (Figure 6.5). Although the existing active samplers are likely impractical for child subjects, the PAAS can be used to assess the allergen exposures of children, which are

likely specific as was demonstrated above, and hence create opportunities to understand the mechanisms of the disease expressions in early life.

6.2. Description of the PAAS

The PAAS can be used to collect large airborne particles such as aeroallergens including mite fecal particles, cedar pollens and fungal spores with diameters ranging 10-40, 25-60 and 2-60 μm, respectively (Tovey et al., 1981; Kitamura et al., 2005; Al-Doory & Domson, 1984). In the PAAS, passive samplings by means of gravitational settling are assumed for relatively large allergenic particles. The sampler is designed to collect large airborne particles on the horizontal collection surface by gravitational settlings. Therefore, the particle collection surface needs to be continuously directed upward to prevent distortion of the measurement results by inclination of the sampler. In the PAAS, this was achieved by a structure resembling a gimbal, which maintains the substrate holder continuously oriented upward (Figures 6.6 and 6.7). Consequently, the sampler can be used as a personal sampler continuously subjected to inclination and/or movement.

The PAAS consists of two planetary rings in different sizes, which enables the substrate holder to rotate in all directions. A particle collection substrate is placed on the filter holder, covered by a protective mesh, and tightened with a stainless filter holder cap. The substrate holder is attached by an inner rotating shaft extending to the inner ring, and the inner ring is attached by an outer rotating shaft extending to the protective outer shell. The inner rotating shaft is oriented at an angle of 90 degrees relative to that of the outer shaft. An underlying structure resembling a gimbal enables the particle collection surface to be continuously directed upward regardless of

inclination of the sampler. To collect airborne particles around the human breathing area, the human subject should wear the passive sampler around his or her neck (Figure 6.8).

6.3. Proposed applications of the PAAS

6.3.1. Microscopic methods

Airborne coarse particles including aeroallergens collected by the PAAS can be analyzed by microscopic methods. For instance, cedar pollens, major aeroallergens inducing allergic rhinitis and conjunctivitis in Japan, collected by the PAAS, can be analyzed by optical microscopes. In general, the Durham pollen samplers (Durham, 1946) are most commonly used to collect cedar pollens in Japan. In this method, cedar pollens collected on a glycerinated glass slide are stained by gentian violet and observed by optical microscopes within a square area of 18 mm × 18 mm (= 320 mm^2) of the slide to enumerate pollen counts. In a similar fashion, the pollens collected on the substrate having a diameter of 22 mm (= 380 mm^2) of the PAAS can be enumerated by optical microscopes. It should be stated the PAAS conforms to the Durham pollen sampler in terms of particle collection surfaces subjected to microscopic observation.

Furthermore, various types of microscopic methods might be possible depending on the types of biological particles to be analyzed. For instance, Griffiths & DeCosemo (1994) reviewed various kinds of microscopic methods including fluorescent and phase-contrast microscopes to analyze biological particles, and the methods they reviewed might be directly applicable to allergenic particles collected by the PAAS. The particles collected by the PAAS can be microscopically observed and analyzed to quantitate air concentrations of target aeroallergens. The allergenic

particles collected by the PAAS are immunostained by antigen-antibody reactions while those non-allergenic are not stained (Figure 6.9). The immunostained particles were observed by biological and/or fluorescent microscopes depending on types of staining materials. The microscopic images can be processed based on color information since only allergenic particles are stained to a particular color. Furthermore, several kinds of allergens can be analyzed at a time by the multistaining methods.

6.3.2. Bulk methods

If the amounts of allergens collected by the PAAS are sufficient, bulk analyses are also feasible. Allergenic substances extracted from the collection substrates can be analyzed by commonly used immunoassay techniques such as ELISA. The culture techniques might be another alternatives to measure the number of viable biological particles collected by the PAAS although these methods are incapable of sizing the collected particles. It should be reminded the particle size information is essential to convert the amounts passively collected to the concentrations in air. Nevertheless, the culture methods have potential as analytical methods for the PAAS since the PAAS conforms to the historically used gravity settling culture plate methods in terms of particle collection mechanisms. Although the gravity settling plate methods have not been used for the personal samplings partly due to difficulty in keeping particle collection surface continuously directed upward regardless of inclination of the sampler, the PAAS can be used for the purpose of the personal samplings because of its characteristic features. For instance, viable fungal spores collected by the PAAS can be cultured and enumerated for the colony forming unit. In our ongoing study, the fungal spores collected on the substrate of the PAAS were extracted in ultrapure water

to make fungal suspensions. Hereafter, the fungal suspensions were filtered on membrane filters with larger diameters to ease counting the cultured colonies. The details of the cultured methods to analyze viable fungi collected by the PAAS will be described in our future report.

References

Al-Doory, Y., & Domson, J. F. (1984). *Mould Allergy*, Philadelphia, Lea and Febiger.

Durham, O. C. (1946). The volumetric incidence of atmospheric allergens. IV. A proposed standard method of gravity sampling, counting, and volumetric interpolation of results. *Journal of Allergy, 17*, 79-86.

Ferro, A. R., Kopperud, R. J., & Hildemann, L. M. (2004). Elevated personal exposure to particulate matter from human activities in a residence. *Journal of Exposure Analysis and Environmental Epidemiology, 14*, S34-S40.

Griffiths, W. D., & DeCosemo, G. A. L. (1994). The assessment of bioaerosols: A critical review. *Journal of Aerosol Science, 25*, 1425-1458.

Halken, S. (2003). Early sensitization and development of allergic airway disease – risk factors and predictors. *Paediatric Respiratory Reviews, 4*, 128-134.

Holt, P. G., Macaubas, C., Stumbles, P. A., Sly, P. D. (1999). The role of allergy in the development of asthma. *Nature, 402*, 12-17.

Irie, T., Yoshizawa, S., Sugawara, F., & Masada, K. (1981). On the dispersion range of large particles generated within room. *Journal of Society of Powder Technology, Japan, 18*, 909-914 (in Japanese).

Kitamura, T., Shiomori, T., Fujimura, T., & Suzuki, H. (2005). Allergy (1) Nasal allergy by pollen. *Journal of Aerosol Research, 20*, 54-57 (in Japanese).

Platts-Mills, T. A. E., Rakes, G., Heymann, P. W. (2000). The relevance of allergen exposure to the development of asthma in children. *Journal of Allergy and Clinical Immunology, 105*, S503-S508.

Sporik, R., Platts-Mills, T. A. E. (2001). Allergen exposure and the development of asthma. *Thorax, 56*, ii58-ii63.

Tovey, E. R., Chapman, M. D., & Platts-Mills, T. A. E. (1981). Mite faeces are a major source of house dust allergens. *Nature, 289*, 592-593.

Table 6.1

Specifications of the personal aeroallergen sampler (PAAS)

Model	Personal Aeroallergen Sampler (PAAS)
Target substances	Large airborne particles including aeroallergens (cedar pollens, fungi, house dust mite, and so on)
Power source	n/a (passive method)
Dimensions	50 mm (w) × 40 mm (d) × 40 (h) mm
Diameter of the collection surface	25 mm
Weight	Approximately 50 g

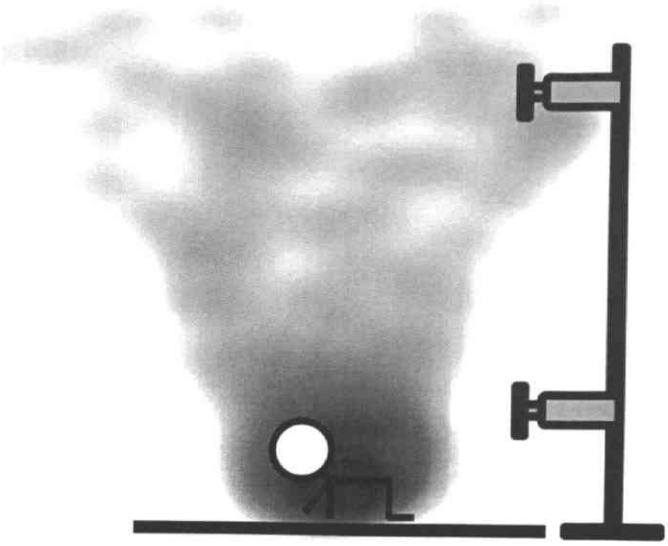

Figure 6.1. Schematic diagram of an error in assessing the personal exposure to resuspended house dusts by fixed point monitoring.

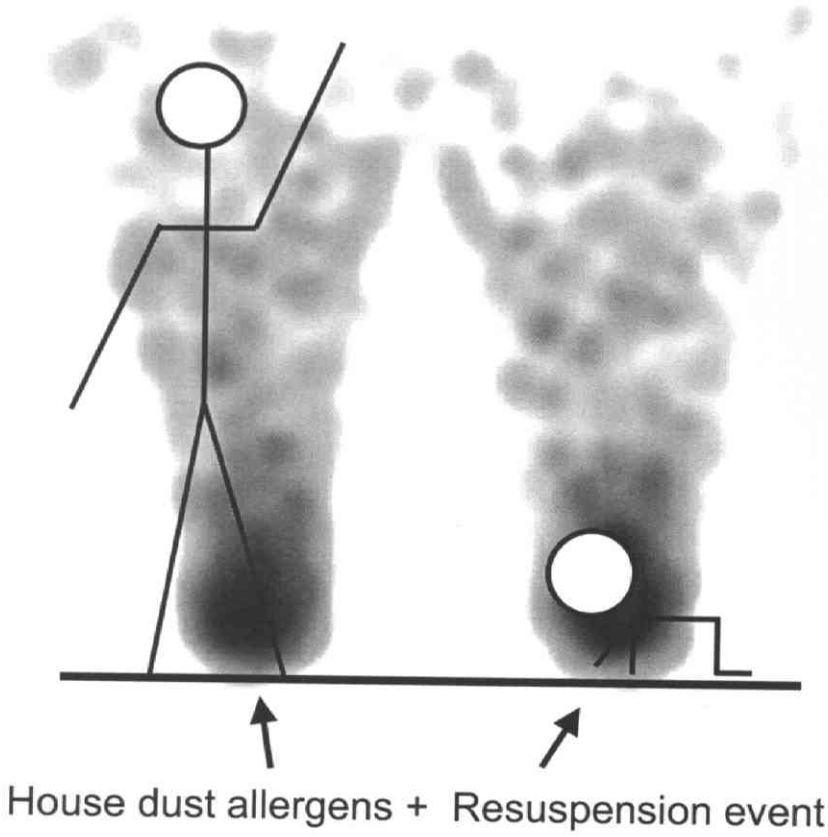

Figure 6.2. Schematic diagram of the child's exposure to resuspended house dust allergens.

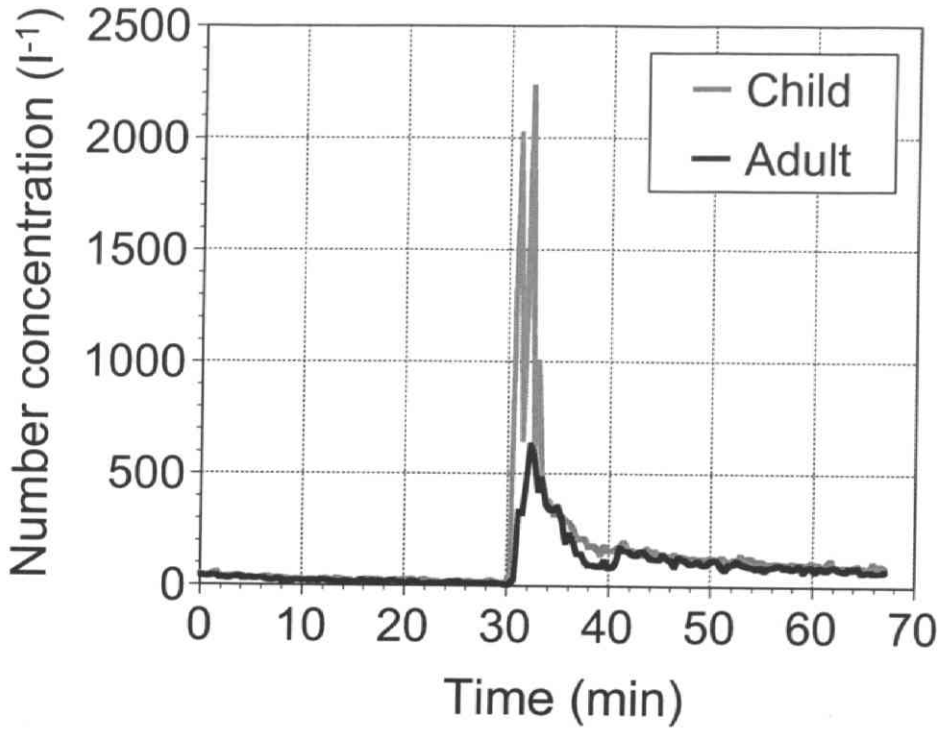

Figure 6.3. An example of the time-course concentrations of the >5 μm particles in adult and child breathing zones in a same room. The house dust resuspension event was undertaken for 3 min approximately at a time of 30 min.

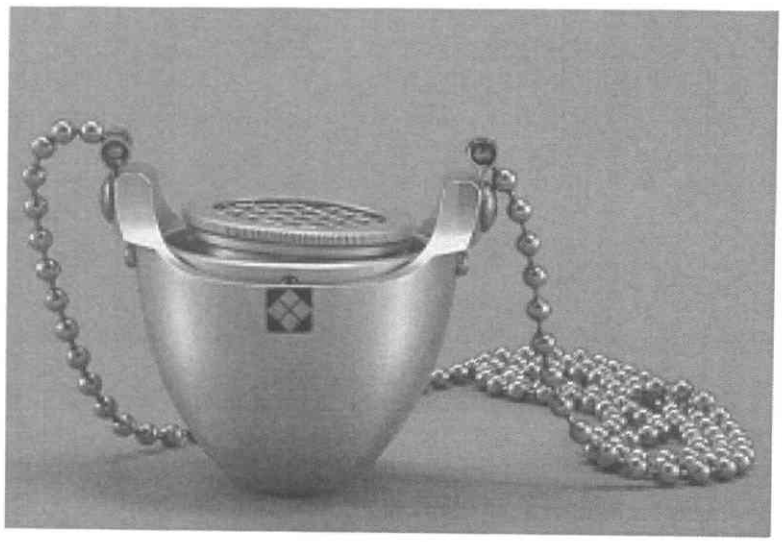

Figure 6.4. Personal aeroallergen sampler (PAAS).

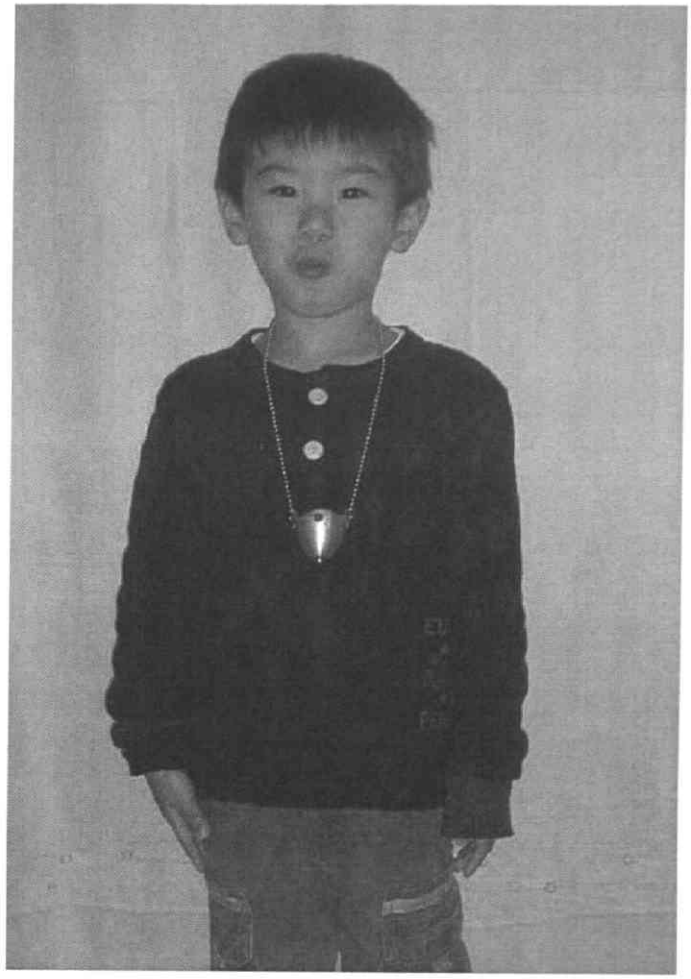

Figure 6.5. The PAAS worn by a child.

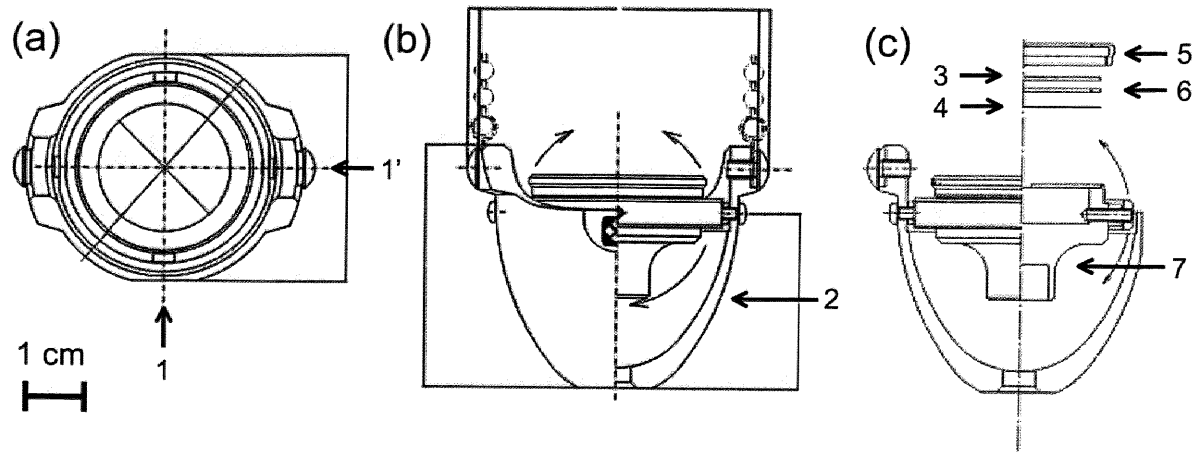

Figure 6.6. Schematic diagrams of the personal aeroallergen sampler (PAAS): (a) overhead view, (b) front view, and (c) inside view. 1, 1'- axes of the gimbal; 2- protective outer shell; 3- protective stainless mesh; 4- collection substrate; 5- substrate holder cap; 6- Teflon ring; 7- substrate holder body.

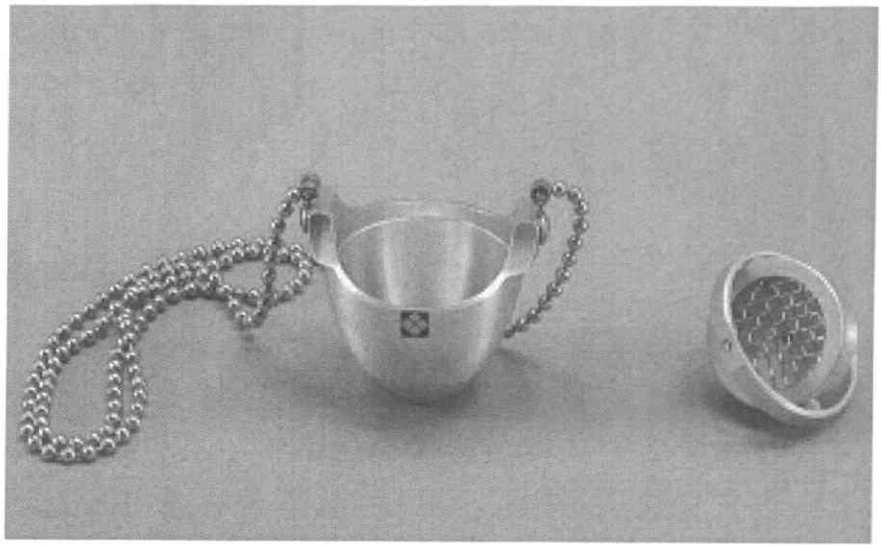

Figure 6.7. Personal aeroallergen sampler (PAAS) composed of the protective outer shell (left) and gimbal-like substrate holder (right).

Figure 6.8. Personal aeroallergen sampler (PAAS) in use.

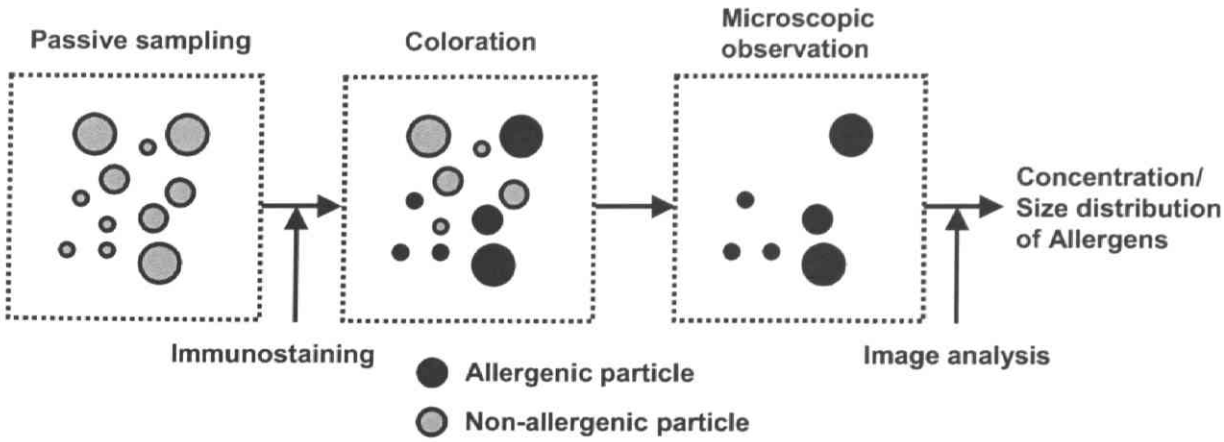

Figure 6.9. Schematic diagram of the microscopic analysis of allergen particles collected the PAAS.

CHAPTER 7.
Microscopic method to quantify airborne coarse particles collected by the PAAS (PAAS-OPM)

CHAPTER 7. Microscopic method to quantify airborne coarse particles collected by the PAAS (PAAS-OPM)

7.1. Objectives in the thesis

The purpose of this chapter is to evaluate the particle collection velocities onto the PAAS. The particle collection velocities were characterized by microscopic observations of the particles collected by the collocated passive and active samplers, i.e., the PAAS and the Institute for Occupational Medicine (IOM) personal sampler, respectively. The OPM, for which the characteristic features have been demonstrated in the previous chapters, was used to analyze the numbers and sizes of the particles collected by both methods. By characterizing the particle collection velocities by the PAAS, the conversion from the amounts of the particles collected by the PAAS to the concentrations in air becomes feasible.

7.2. General backgrounds

Passive samplers are devices to collect airborne substances by naturally occurred mass transfers. The passive samplers are convenient for personal air monitoring, and have been widely used because of simplicity of handling, (e.g., Yanagisawa & Nishimura, 1982; Shields & Weschler, 1987; Levy et al., 1998; Shinohara et al., 2004). While the passive sampling methods have been established for gaseous substances such as nitrogen oxides or volatile organic compounds, the methods are still under development for airborne particles. This is primarily due to complexity

to convert the amounts passively collected to the concentrations in air. Since ambient aerosol particles are generally heterogeneous in terms of size, shape and density, it is difficult to determine contributions of each particle transport mechanisms including the Brownian diffusion, gravitational settling, and inertial or electrostatic depositions. Therefore, unique values of mass transfer coefficients to convert the amounts passively collected to the concentrations in air are hardly assumed for ambient aerosol particles.

Nevertheless, various types of passive aerosol samplers have been challenged in the past. For instance, methods using an electret-based material (Brown et al., 1994a, 1994b, 1995; Thorpe, et al., 1999), horizontal and vertical sticky substrates (Vinzents, 1996), and a particle deposition velocity model in conjunction with the microscopic observation (Wagner & Leith, 2001a, 2001b, 2001c) have been reported. As described above, a difficulty to convert the amounts passively collected to the concentrations in air lies in lack of information of particle motions in air. Transport mechanisms of the particles in air are dominated by their physical properties such as size, shape and density. Therefore, the microscopic observations to capture their geometrical information are essential to predict their motions in air. Whereas the particle densities and dynamic shape factors might remain to be unknown even with the microscopic observations, the microscopic methods are useful if these variables can be sufficiently presumed for measured particles. For instance, these variables can be adequately assumed for aerosol species from certain sources under occupational environments (Wagner & Leith, 2001c).

We have recently developed the personal aeroallergen sampler (PAAS), a passive personal sampler for airborne coarse particles (Figure 6.4). The PAAS is designed to collect airborne coarse particles on a horizontal collection surface by means

of inertial and/or gravitational depositions. The PAAS consists of two planetary rings in different sizes in which a substrate holder can rotate in all directions. A particle collection substrate is placed on the filter holder, covered by a protective mesh, and tightened by a stainless filter holder cap. While the substrate holder is attached by an inner rotating shaft extending to an inner ring, the inner ring is attached by an outer rotating shaft extending to a protective outer shell. The inner rotating shaft is oriented at an angle of 90 degree relative to that of the outer shaft. An underlying structure resembling a gimbal enables particle collection surface continuously directed upward regardless of inclination of the sampler.

The purpose of this study is to characterize particle collection velocities by the PAAS by comparison with an existing active sampling method. To analyze the particle size distributions obtained by both methods, a line-sensing optical microscope (OPM) (Yamamoto et al., 2002, 2004) was employed to observe the particles collected on the sampler's substrates. The particle size distributions obtained by these two methods were compared to calculate the particle collection velocities by the PAAS. Furthermore, the experimental particle deposition velocities were compared with the theoretical velocities calculated by an existing particle dry deposition model. In this study, airborne particles with diameters ranging 10-100 μm were selected for the analyses since these coarse particles include aeroallergens such as mite fecal pellets, cedar pollens and fungal spores having diameters of 10-40, 25-60 and 2-60 μm, respectively (Tovey et al., 1981; Kitamura et al., 2005; Al-Doory & Domson, 1984), and are important from the aspect of allergic airway diseases.

7.3. Methods

7.3.1. Description of the PAAS

Schematic diagrams of the PAAS are shown in Figure 6.6. Briefly, the sampler consists of two planetary rings in different sizes which enable a substrate holder to rotate in all directions (Figure 6.6 (a)). A mixed cellulose ester membrane (MCE) filter (25 mm filter diameter, 0.8 μm pore size; SKC Inc., PA, USA), a collection substrate, was placed with an absorbent cellulose pad on the substrate holder, covered by a Teflon ring and a protective stainless mesh (2.09 mm mesh aperture, 0.45 mm wire diameter, 68 % mesh opening), and tightened by a stainless filter holder cap (Figure 6.6 (c)). To prevent reentrainment of the collected particles from the substrate, the substrates were immersed in mineral oil before loading on the substrate holder. The substrate holder is attached by an inner rotating shaft extending to an inner ring, and the inner ring is attached by an outer rotating shaft extending to a protective outer shell. The inner rotating shaft is oriented at an angle of 90 degree relative to that of the outer shaft. An underlying structure resembling a gimbal enables the particle collection surface to be continuously directed upward regardless of inclination of the sampler. Human subjects should wear the PAAS around his or her neck to collect airborne particles around his or her breathing areas (Figure 6.8).

7.3.2. Sampling procedures

To evaluate the particle collection characteristics by the PAAS, an active sampler was collocated for comparison. The Institute for Occupational Medicine (IOM) personal sampler (Mark & Vincent, 1986) (SKC Inc., PA, USA) connected to a portable pump (MP-Σ500; Sibata Scientific Technology Ltd., Tokyo, Japan) was used as

an active sampler. The IOM sampler was used as a reference active sampling method because it is the most commonly used personal inhalable sampler that conforms well to the inhalable particulate matter sampling criterion given by the American Conference of Government Industrial Hygienists (ACGIH, 2003). The MCE filter was loaded in a filter holder of the IOM sampler. A sampling flow rate was adjusted at 2 l min^{-1} as instructed by the manufacturer. Ten collocated personal samplings for durations ranging from 6 hr to 6 days were taken indoors and/or outdoors. In case the collocated samplings were taken more than 8 hr, the filter of the active sampler was replaced with new one every 8-12 hr to prevent the particle overload. Although the human subjects should wear the PAAS around his or her necks, both active and passive samplers were attached to a handbag during the personal samplings to reduce the burden for the human subject to carry the active sampler. The collocated personal samplings were taken during commuting in trains, staying outdoors and in the offices or houses in the central part of Tokyo in August to December 2005.

To roughly assess wind effects on particle collection characteristics by the PAAS, the collocated outdoor samplings were taken 5 times on relatively windy days in December 2005. Both the PAAS and IOM sampler were placed outside the sixth floor room of the building (approximately 20 m from the ground level) of the University of Tokyo in Bunkyo-ku, located in the central part of Tokyo. The collocated outdoor samplings were taken for 5-23 hr. Information of wind velocities during the sampling periods was obtained at the nearest monitoring station of the Bureau of Environment, Tokyo Metropolitan Government as a reference. The monitoring station is located approximately 2 km north of the building of the University of Tokyo. It should be stated wind velocities measured at the monitoring station did not necessarily represent

those at the sampling point of the PAAS. Instead, the information was simply referred to signify an effect of wind on particle collection characteristics by the PAAS for the outdoor samplings on relatively windy days.

7.3.3. Microscopic method

An optical microscope with a line sensor camera (OPM) (Dot Analyzer DA-6100/LS; Oji Scientific Instruments, Hyogo, Japan) was used to capture the image of particles collected on the substrates. Its line sensing mechanism with a linear motor actuating slide enabled broad range observations of target materials (approximately 6 mm × 16 mm) at a time. Captured images were imported to a graphic software (Adobe Photoshop 4.0 LE, Adobe System Inc.) to segment the images into black and white pixels (pixel pitch = 2.7 μm) and then introduced to an image analysis software (DA-6000 bundled with the Dot Analyzer DA-6100/LS; Oji Scientific Instruments, Hyogo, Japan) to process sizes and numbers of collected particles. The particles deposited on the substrate surface with an area of A = 200-300 mm^2, i.e., approximately 40-60 % of the substrate surface, were randomly sensed and observed by the OPM. Fibrous substances were not counted because these are unlikely allergenic and atmospheric behaviors are likely different from those of spherical particles. The sizing accuracy of the OPM method was characterized by observing the black colored polystyrene latex particles with 10 and 100 μm diameters (Duke Scientific Corp., CA, USA) of the National Institute of Standards and Technology (NIST) traceable (Table 3.1). These analytical results were previously reported in Chapter 3.

7.4. Model

The theoretical particle deposition velocities calculated based on a dry deposition model developed by Kim et al. (2000) were compared with the experimental results obtained by the PAAS. In their model, the dry deposition velocities, V_d, due to gravitational settling and inertial deposition caused by atmospheric turbulence were calculated for particles with diameters ranging from 10 to 100 μm. In their model, the value of V_d is given by a following equation:

$$V_d = V_g + V_i, \tag{7.1}$$

where V_g is the terminal settling velocity, and V_i is the inertial velocity of the particles.

In this study, the value of V_g was calculated by a following equation (Hinds, 1999):

$$V_g = \frac{\rho_0 d_a^2 g}{18\eta}, \tag{7.2}$$

where ρ_0 (= 1.0 g cm^{-3}) is the standard particle density, d_a is the aerodynamic equivalent diameter of the particle, g (= 980 cm s^{-2}) is the acceleration of gravity, and η (= 1.8×10^{-5} Pa s) is the viscosity of air. Here the value of d_a was estimated by the projected area diameter of the particle, d_{PA}, characterized by the microscopic observation, and calculated by a following empirical equation (Noll et al., 1988):

$$d_a = \frac{1}{1.39} d_{PA}, \tag{7.3}$$

Although the actual conversion factor was not measured, the average d_{PA}/d_a ratio of 1.39 reported by Noll et al. (1988) and Noll & Fang (1989) was tentatively used in this study.

Meanwhile, the value of V_i, was computed by a following equation (Kim et al., 2000):

$$V_i = u^* \eta_{dl}, \tag{7.4}$$

where η_{dI} is an eddy deposition efficiency associated with particle inertia, and u^* is the friction velocity of air. Although the friction velocity was not measured in this study, the values of $u^* = 0$, 10, 20, 30, 40, 50 cm s^{-1} were arbitrarily assigned. The value of η_{dI} is, on the other hand, given by a following equation (Kim et al., 2000):

$$\eta_{dI} = 10^{-3/\mathrm{Stk}_e}, \tag{7.5}$$

where Stk_e is the eddy Stokes number defined by a following equation:

$$\mathrm{Stk}_e = \frac{V_g u^{*2}}{g\nu}, \tag{7.6}$$

where ν is the kinematic viscosity of air (= 0.156 cm^2 s^{-1}).

In this study, the theoretical values of V_d for size-fractionated particles having size intervals of d_{PA} = 10-20, 20-30, 30-50 and 50-100 μm were calculated to compare with the experimental results. To obtain a representative value of the V_d within the particle diameter interval between a and b, $(V_d)_{ab}$, the values of V_d of each observed particle were integrated over its size range and divided by the observed number of the particles. Therefore, the equation is given by:

$$(V_d)_{ab} = \frac{\sum_{i=1}^{N} V_d(d_{\mathrm{PA},i})}{N}, \qquad \text{for } a < d_{\mathrm{PA},i} < b \tag{7.7}$$

where N is the number of observed particles, and $V_d(d_{PA,i})$ is the deposition velocity for the i th particle having a diameter of $d_{PA,i}$. The value of $V_d(d_{PA,i})$ was calculated by Eqs. (7.1)-(7.6) based on information of $d_{PA,i}$ characterized by the microscopic observation. The number of observed particles, N, was characterized by the microscopic observation, too.

7.5. Results and discussion

7.5.1. Particle collections by the PAAS and IOM sampler

The microscopic images of captured particles on the substrates of the active and passive samplers, i.e., the IOM sampler and PAAS, respectively, are shown in Figure 7.1. The coverage area fractions by the particles collected on the collection substrates of the PAAS were relatively small. For instance, the particle coverage area fraction was 0.68 % for the 6-day personal sampling. Therefore, the particle overlapping on the collection substrate was expected to be insignificant for the personal samplings for durations up to a week at least. Approximately 16-2100 particles with diameters larger than 10 μm were counted on each collection substrate with a surface area of A = 200-300 mm^2 of the PAAS. An example of particle size distributions by the active and passive methods is shown in Figure 7.2. In Figure 7.3, the particle numbers collected by the active and passive methods, i.e., n_a and n_p, respectively, are plotted for the personal and outdoor samplings. The particle numbers collected by the passive sampler were generally smaller than those by the active sampler. The ratios of the particle numbers collected by the PAAS to the IOM sampler for the personal samplings were 1.8, 4.3, 9.2 and 28 % for the particles with diameters of 10-20, 20-30, 30-50 and 50-100 μm, respectively. Meanwhile, the ratios tended to be larger for the outdoor samplings on relatively windy days, i.e., 6.6, 15, 42 and 116 % for the particles with diameters with 10-20, 20-30, 30-50 and 50-100 μm, respectively, indicating higher particle collection efficiencies by the PAAS in the outdoor samplings than in the personal samplings.

Above-mentioned results indicate the particle collection velocities by the PAAS were influenced by wind. According to the Bureau of Environment, Tokyo

Metropolitan Government, minimum, maximum, mean, and median wind velocities measured at the nearest monitoring station from the sampling point by the PAAS were 0.3, 11.4, 5.5, and 5.7 m s^{-1}, respectively, during the outdoor samplings. Meanwhile, although the indoor air velocities were not measured in this study, the velocities typically observed indoors are much lower than the abovementioned outdoor air velocities. For instance, Matthews et al. (1989) reported indoor air velocities at a level of 10 cm s^{-1} in occupied and unoccupied dwellings. Since the majority of the time was spent indoors for the personal samplings in this study, i.e., approximately 85 % excluding the time spent for commuting, the wind velocities experienced during the personal samplings were expected to be much lower than those observed outdoors. As will hereinafter be described in detail, the difference of the wind velocities might cause the observed discrepancy between the particle collection velocities in the outdoor and personal samplings. Nevertheless, good correlations between the two methods were observed for the personal samplings, i.e., the squares of the correlation, R^2, of 0.9498, 0.9372, 0.9480 and 0.8457 for particles with diameters of 10-20, 20-30, 30-50 and 50-100 μm, respectively, suggesting usability of the PAAS for the purpose of the personal samplings of airborne coarse particles.

7.5.2. Particle deposition velocities onto the PAAS

Provided the particle concentrations obtained by the active sampling method represent the true concentrations in air, the ratio of the particle numbers collected by the passive to active methods, i.e., n_p/n_a, should be equal to the ratio of the particle deposition velocity onto the passive sampler to the face velocity of air through the filter of the active sampler, i.e., V_d/V_0. Nevertheless, the particle collection efficiency of the

active sampler, i.e., the IOM sampler, is known to vary depending on the particle size and conform to the inhalable fraction sampling criterion IF(d_a) given by the ACGIH (2003):

$$\mathrm{IF}(d_a) = 0.5(1 + \exp(-0.06 d_a)), \qquad \text{for } U_0 \leq 1.0 \text{ m s}^{-1} \tag{7.8}$$

where d_a is the aerodynamic diameter in μm and U_0 is the ambient air velocity. To relate the particle deposition velocity onto the passive sampler to the absolute particle concentration in air, the true number of particles which should be contained in the volume of air collected by the active method, n_0, needs to be calculated using a following equation:

$$n_0 = \frac{n_a}{\mathrm{IF}(d_a)}, \tag{7.9}$$

Therefore, the particle deposition velocity onto the PAAS relative to the absolute particle concentration in air is represented by a following equation:

$$V_d = V_0 \frac{n_p}{n_0}, \tag{7.10}$$

Meanwhile, the face velocity of air through the filter of the IOM sampler, V_0, is given by a following equation:

$$V_0 = \frac{Q}{A_e}, \tag{7.11}$$

where Q (= 2 l min^{-1}) is the sampling flow rate, and A_e is the effective particle deposition area on the filter. Since the 19 mm diameter area of the filter was exposed to the airstream, the value of A_e for the IOM sampler was calculated to be 280 mm^2. Therefore, the value of V_0 in Eq. (7.11) was calculated to be 12 cm sec^{-1}.

In this study, the values of IF(d_a) were calculated for each particle size interval of d_{PA} = 10-20, 20-30, 30-50 and 50-100 μm, i.e., d_a = 7.2-14, 14-22, 22-36, 36-72 μm by Eq. (7.3). To obtain a representative value of the IF(d_a) within the particle diameter

interval between a and b, $(\mathrm{IF}(d_a))_{ab}$, the values of $\mathrm{IF}(d_a)$ of each observed particle were integrated over its size range and divided by the observed number of the particles. Therefore, the equation is given by:

$$(\mathrm{IF}(d_a))_{ab} = \frac{\sum_{i=1}^{N} \mathrm{IF}(d_{a,i})}{N}, \qquad \text{for } a < d_{a,i} < b \tag{7.12}$$

where N is the number of observed particles, and $\mathrm{IF}(d_{a,i})$ is the $\mathrm{IF}(d_a)$ for the i th particle having a diameter of $d_{a,i}$. By combining Eqs. (7.9)-(7.12), the value of $(V_d)_{ab}$ is given by a following equation:

$$(V_d)_{ab} = V_0 (\mathrm{IF}(d_a))_{ab} \frac{n_p}{n_a}, \tag{7.13}$$

The means of $(V_d)_{ab}$ of each data set weighted by the observed particle numbers were calculated to obtain representative values of V_d for each particle size interval, i.e., d_{PA} = 10-20, 20-30, 30-50 and 50-100 μm.

Following the abovementioned calculation procedures, the experimental values of V_d = 0.17, 0.35, 0.66 and 1.6 cm s^{-1} were obtained for the personal samplings while the values of V_d = 0.63, 1.2, 3.0 and 7.7 cm s^{-1} were calculated for the outdoor samplings for particles with size intervals of d_{PA} = 10-20, 20-30, 30-50 and 50-100 μm, respectively. It should be stated the values for the outdoor samplings were calculated for the purpose of reference since Eq. (7.8) was limited to the case of $U_0 \leq 1.0$ m s^{-1}. Since the ambient air velocities during the outdoor samplings were larger than 1.0 m s^{-1} as described above, the values calculated for the outdoor samplings are likely inaccurate.

7.5.3. Experimental and theoretical deposition velocities

In Figure 7.4, the experimental values of V_d are shown with the theoretical

values calculated by the dry deposition model. The figure illustrates the experimental velocities for the personal samplings were lower than the theoretical velocities. Nevertheless, the profile of the experimental results of V_d obtained by the personal samplings was similar to that of the theoretical results calculated with an assumption of the Stokes settling, i.e., $u^* = 0$ cm sec^{-1}, suggesting inertial deposition due to atmospheric turbulence was insignificant for the personal samplings. Although many studies (e.g., Noll & Fang, 1989; Kim et al., 2000) reported the friction velocities of air in the open atmospheres at a level of $u^* = 30$ cm s^{-1}, the velocities are much lower indoors. For instance, Matthews et al. (1989) measured indoor air velocities at a level of 10 cm s^{-1} in occupied and unoccupied dwellings. Since the friction velocity is defined as a square root of a product of vertical and horizontal wind velocity fluctuations, the values of u^* measured indoors are expected to be much lower than 10 cm s^{-1}. Furthermore, since people spend the majority of the time indoors (Jenkins et al., 1992), the effect of air turbulence on the particle collection by the PAAS is expected to be negligible for the purpose of the personal samplings. In this study, the collocated samplings of the PAAS and IOM sampler were taken indoors in large part of time, i.e., approximately 85 % excluding the time spent for commuting.

Meantime, the lower experimental values observed by the PAAS were expected due to the effects of the sampler's geometry. Although the experimental values of V_d were compared with the theoretical values calculated by the dry deposition model by Kim et al. (2000), their model was established based on the particle deposition to a smooth surrogate surface with a sharp leading edge. Since the particle collection substrate was loaded in the hollow of the substrate holder, covered by a protective mesh, and tightened by a stainless filter holder cap in the PAAS (Figure 6.6 (c)), these might

shade the particle deposition flux to the collection substrate. This could cause decrease of the particle collection efficiency by the PAAS.

7.5.4. Concentration calculations

To convert the amounts of particles collected by the PAAS to the concentrations in air, a following general expression can be used:

$$C = \frac{F}{V_d}, \tag{7.14}$$

where C (number cm^{-3}) is the particle number concentration, and F (number cm^{-2} s^{-1}) is the particle number flux to the collection substrate of the PAAS. The values of F in Eq. (14) were obtained by a following equation:

$$F = \frac{n_p}{t}, \tag{7.15}$$

where t (s) is the sampling time, and n_p (number cm^{-2}) is the number of the particles deposited on unit area of the collection substrate. Therefore, the particle concentrations in air are represented by a following equation:

$$C = \frac{n_p}{V_d t}, \tag{7.16}$$

where the values of V_d experimentally obtained by the personal samplings are 0.17, 0.35, 0.66 and 1.6 cm s^{-1} for d_{PA} = 10-20, 20-30, 30-50 and 50-100 μm, respectively. Since theses values were experimentally obtained for the particle groups having certain diameter intervals, the values have to be estimated for each particle size.

To estimate the values of V_d along with the particle size, the theoretical values of V_d were fitted to the experimental data, in which the sampler's geometry was chosen as a fitting parameter. The parameter related to the sampler's geometry, a, was incorporated in Eq. (7.1) under the assumption that the effect of the sampler's geometry

was not dependent on the particle size. Meanwhile, the effect of the atmospheric turbulence was neglected based on the experimental observation that was explained in the previous section. Therefore, the second term of Eq. (7.1), i.e., V_i, was ignored, and the expression to fulfill above-mentioned assumptions is given by:

$$V_d = aV_g, \tag{7.17}$$

By fitting the theoretical calculation to the experimental data, we obtained $a = 0.28$ with $R^2 = 0.9798$. Therefore, a regression equation to estimate the values of V_d along with the particle size is given by:

$$V_d = 0.28V_g, \tag{7.18}$$

where the values of V_g are calculated by Eq. (7.2). The value of d_a in Eq. (7.2) is, on the other hand, calculated by Eq. (7.3) based on information of d_{PA} characterized by the microscopic observation. The values of V_d calculated by these equations are used to convert the number of collected particles to the concentration in air by Eq. (7.16). It should be noted the number of collected particles could be characterized by the microscopic observation, too. The deposition velocities obtained by Eq. (7.18) are plotted along with the particle diameter in Figure 7.5.

In this study, the collocated personal samplings by the PAAS and IOM sampler were taken indoors in large part of time, i.e., approximately 85 % excluding time spent for commuting. Therefore, the above-mentioned equations might not be sufficiently accurate for concentration calculations if the sampling times spent indoors and outdoor, and/or the sampling conditions such as atmospheric turbulence are significantly different from those observed in the present personal sampling experiments. From these viewpoints, future research should further elucidate the effects of atmospheric

turbulence on the particle collection characteristics by the PAAS, for instance, by conducting wind tunnel experiments. Nevertheless, the study demonstrated good correlations between the two methods under the atmospheric conditions we normally encountered in our daily lives, suggesting usability of the PAAS for the purpose of personal samplings.

7.6. Summary and conclusions

The PAAS with a structure resembling a gimbal to enable a particle collection surface continuously directed upward regardless of inclination of the sampler was developed. To evaluate the particle collection characteristics by the PAAS, the particle size distributions obtained by the PAAS were compared with those by the IOM sampler for sampling durations ranging from 5 hr to 6 days. The results showed good correlations between the two methods, suggesting usability of the PAAS for the purpose of the personal samplings of airborne coarse particles such as aeroallergens. The particle deposition velocities experimentally obtained for the personal samplings by the PAAS were 0.17, 0.35, 0.66 and 1.6 cm s^{-1} for particles with d_{PA} = 10-20, 20-30, 30-50 and 50-100 μm, respectively. These experimental values were lower than the theoretical values based on the existing particle dry deposition model, suggesting the effects of the sampler's geometry. Nevertheless, the profile of the experimental values of V_d was similar to that of the theoretical values calculated with an assumption of the Stokes settling, i.e., u^* = 0 cm sec^{-1}, suggesting inertial deposition due to atmospheric turbulence was insignificant. The effect of air turbulence on the particle collection by the PAAS is expected to be negligible for the purpose of personal samplings since people spend the majority of the time in buildings where the air turbulence is

sufficiently low. Unlike existing active samplers, the PAAS is convenient for personal air monitoring because of its simplicity of handling. Therefore, it can be used for a variety of epidemiological studies to investigate relationships between aeroallergen exposures and allergic airway diseases.

References

American Conference of Governmental Industrial Hygienists (2003). *TLVs® and BEIs®*. Cincinnati, Ohio, ACGIH.

Al-Doory, Y., & Domson, J. F. (1984). *Mould allergy*, Philadelphia, Lea and Febiger.

Brown, R. C., Hemingway, M. A., Wake, D., & Thompson, J. (1995). Field trials of an electret-based passive dust sampler in metal-processing industries. *Annals of Occupational Hygiene, 39*, 603-622.

Brown, R. C., Wake, D., Thorpe, A., Hemingway, M. A., & Roff, M. (1994a). Theory and measurement of the capture of charged dust particles by electrets. *Journal of Aerosol Science, 25*, 149-163

Brown, R. C., Wake, D., Thorpe, A., Hemingway, M. A., & Roff, M. (1994b). Preliminary assessment of a device for passive sampling of airborne particulate. *Annals of Occupational Hygiene, 38*, 303-318.

Hinds, W. C. (1999). *Aerosol technology: Properties, behavior, and measurement of airborne particles* (2nd ed.). New York, Wiley.

Jenkins, P. L., Phillips, T. J., Mulberg, E. J., & Hui, S. P. (1992). Activity patterns of Californians: Use of and proximity to indoor pollutant sources. *Atmospheric Environment, 26A*, 2141-2148.

Kim, E., Kalman, D., & Larson, L. (2000). Dry deposition of large, airborne particles onto a surrogate surface. *Atmospheric Environment, 34*, 2387-2397.

Kitamura, T., Shiomori, T., Fujimura, T., & Suzuki, H. (2005). Allergy (1) Nasal allergy by pollen. *Journal of Aerosol Research, 20*, 54-57 (in Japanese).

Levy, J. I., Lee, K., Spengler, J. D., & Yanagisawa, Y. (1998). Impact of residential nitrogen dioxide exposure on personal exposure: An international study. *Journal of the Air & Waste Management Association, 8*, 553-560.

Mark, D., & Vincent, J. H. (1986). A new personal sampler for airborne total dust in workplaces. *Annals of Occupational Hygiene, 30*, 89-102.

Matthews, T. G., Thompson, C. V., Wilson, D. L., Hawthorne, A. R., & Mage, D. T. (1989). Air velocities inside domestic environments: An important parameter in the study of indoor air quality and climate. *Environment International, 15*, 545-550.

Noll, K. E., Fang, K. Y. P., & Watkins, L. A. (1988). Characterization of the deposition of particles from the atmosphere to a flat plate. *Atmospheric Environment, 22*, 1461-1468.

Noll, K. E., & Fang, K. Y. P. (1989). Development of a dry deposition model for atmospheric coarse particles. *Atmospheric Environment, 23*, 585-594.

Shields, H. C., & Weschler, C. J. (1987). Analysis of ambient concentrations of organic vapors with a passive sampler. *Journal of Air Pollution Control Association, 37*, 1039-1045.

Shinohara, N., Kumagai, K., Yamamoto, N., Yanagisawa, Y., Fujii, M., & Yamasaki, A. (2004). Field validation of an active sampling cartridge as a passive sampler for long-term carbonyl monitoring. *Journal of the Air & Waste Management Association, 54*, 419-424.

Thorpe, A., Hemingway, M. A., & Brown, R. C. (1999). Monitoring of urban particulate using and electret-based passive sampler. *Applied Occupational and Environmental Hygiene, 14*, 750-758.

Tovey, E. R., Chapman, M. D., & Platts-Mills, T. A. E. (1981). Mite faeces are a major source of house dust allergens. *Nature, 289*, 592-593.

Vinzents, P. S. (1996). A passive personal dust monitor. *Annals of Occupational Hygiene, 40*, 261-280.

Wagner, J., & Leith, D. (2001a). Passive aerosol sampler. I: Principle of operation. *Aerosol Science and Technology, 34*, 186-192.

Wagner, J., & Leith, D. (2001b). Passive aerosol sampler. II: Wind tunnel experiments. *Aerosol Science and Technology, 34*, 193-201.

Wagner, J., & Leith, D. (2001c). Field tests of a passive aerosol sampler. *Journal of Aerosol Science, 32*, 33-48.

Yamamoto, N., Fujii, M., Endo, O., Kumagai, K., & Yanagisawa, Y. (2002). Broad range observation of particle deposition on greased and non-greased impaction surfaces using a line-sensing optical microscope. *Journal of Aerosol Science, 33,* 1667-1679.

Yamamoto, N., Shinozuka, Y., Kumagai, K., Fujii, M., & Yanagisawa, Y. (2004). Particle size distribution quantification by microscopic observation. *Journal of Aerosol Science, 35*, 1225-1234.

Yanagisawa, Y., & Nishimura, H. (1982). A badge-type personal sampler for measurement of personal exposure to NO2 and NO in ambient air. *Environment International, 8*, 235-242.

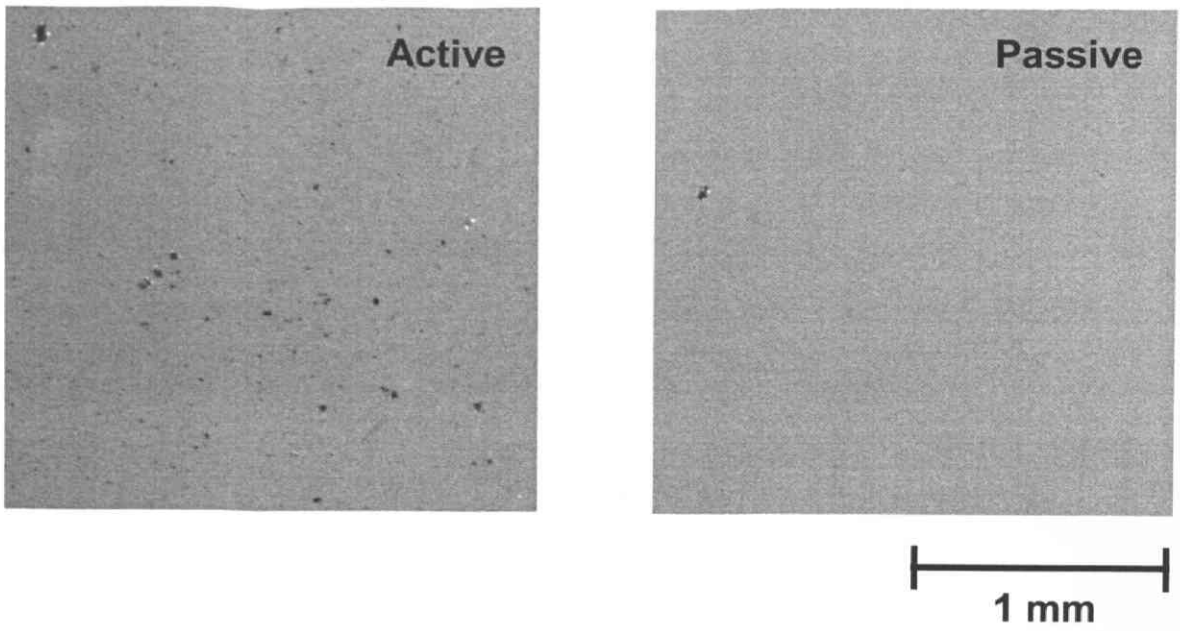

Figure 7.1. Microscopic images of captured particles on the filters of the active (IOM sampler) and passive (PAAS) methods.

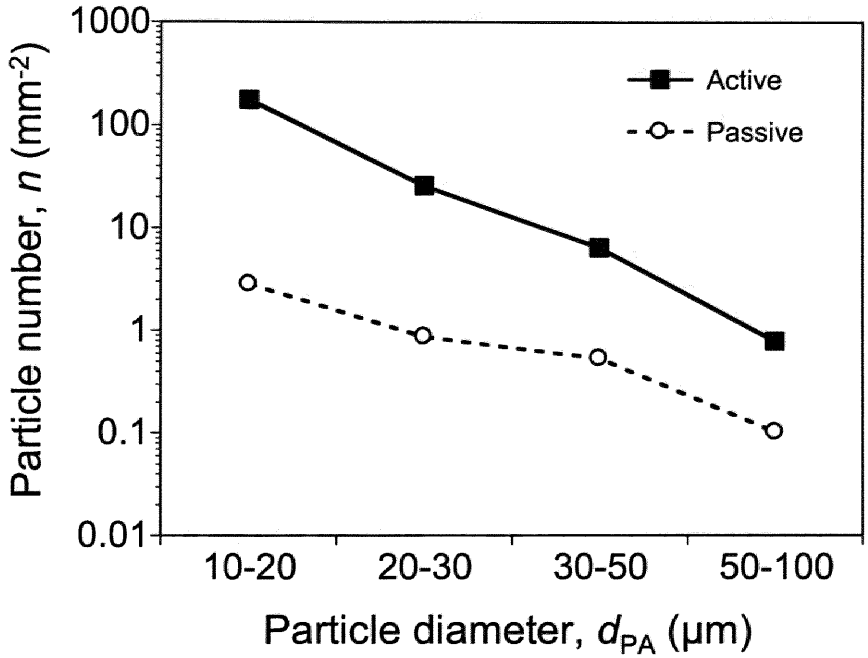

Figure 7.2. An example of size distributions of the particles collected on a unit area of the substrates by the active (IOM sampler) and passive (PAAS) methods.

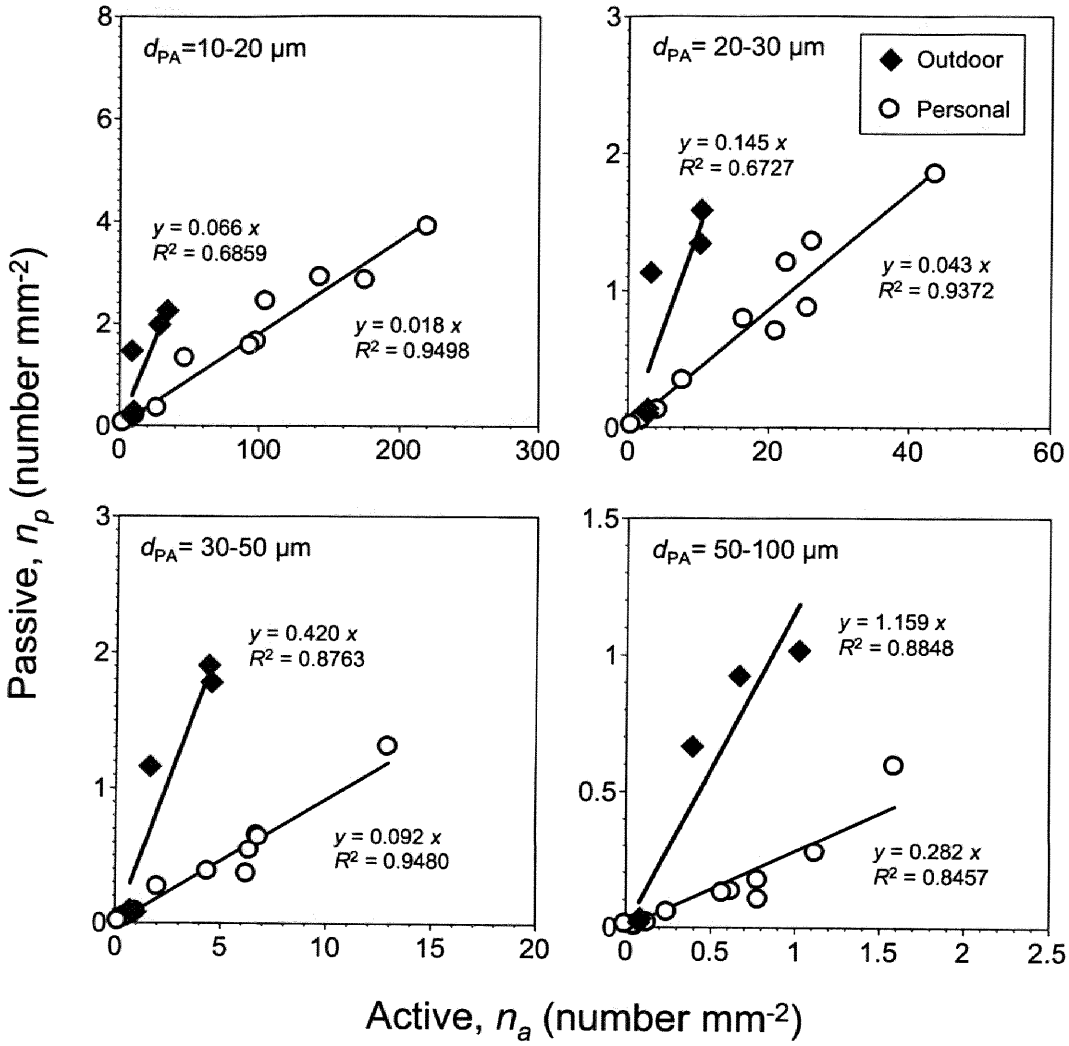

Figure 7.3. Numbers of the collected particles on unit area of the collection substrates by the active (IOM sampler) and passive (PAAS) samplers for the personal and outdoor samplings.

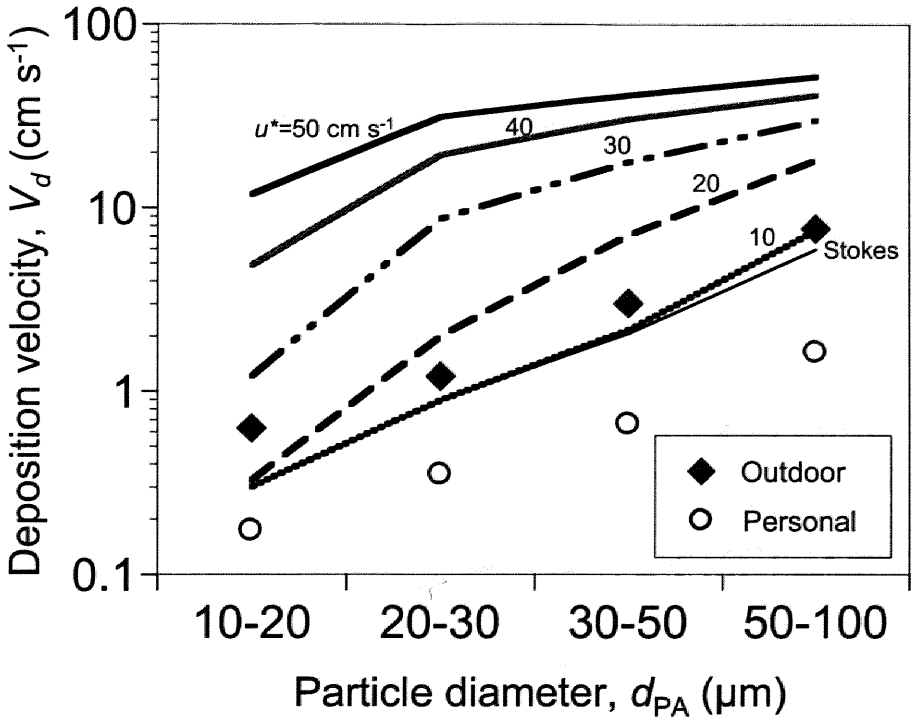

Figure 7.4. Experimental and theoretical deposition velocities of the airborne particles collected by the PAAS for the personal samplings.

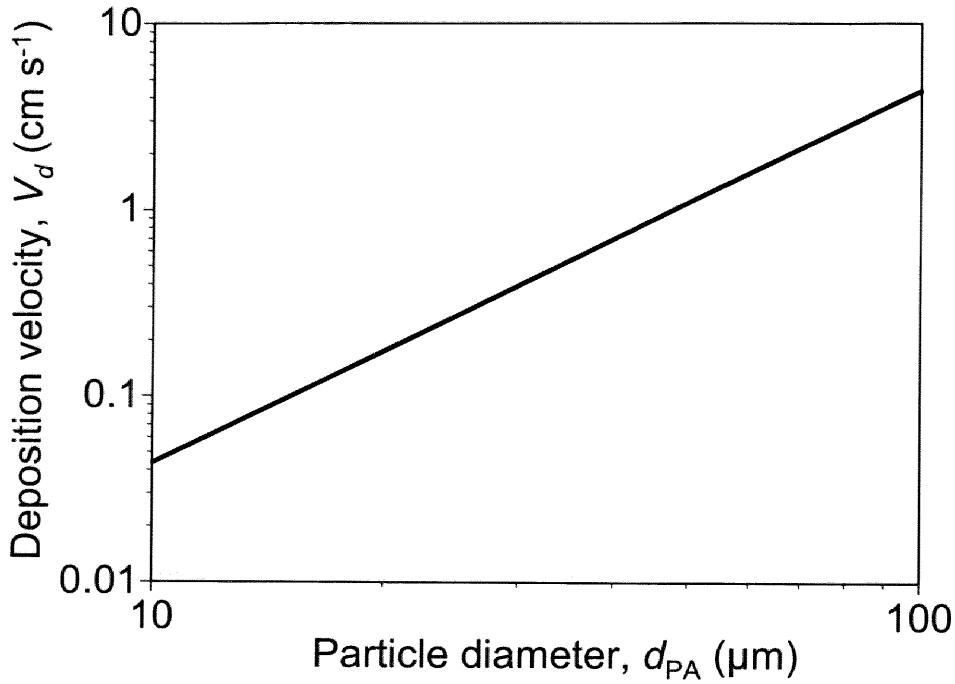

Figure 7.5. Fit result of deposition velocities of the airborne particles collected by the PAAS for the personal samplings.

CHAPTER 8.
Overall summary and conclusions

CHAPTER 8. Overall summary and conclusions

In the first half of this thesis (Chapters 2-5), basic aspects of the OPM for measuring coarse airborne particles were investigated. As was summarized in Chapter 5, the advantages of the OPM method lie in sensitivity in particle detection as well as trueness in particle sizing. For instance, while a practical limit of the sensitivity for weighing most air-sampling filters by electrobalances is 10 μg in general, the sensitivity of microscopic methods is in theory the quantity of each individual particle detected by microscopes. In Chapter 4, we exemplified the sensitivity of the OPM by roughly calculating the particle mass collected by the CI based on the particle number distributions characterized by the OPM. Assuming the spherical particles having unit density, 6.7 μg of the particles was collected on the greased substrates while 3.5 μg was on the non-greased substrates. Since a practical limit of the sensitivity by microbalances is 10 μg, it is apparent the OPM is sensitive to analyze the particle size distributions well below the detection limits of microbalances. Furthermore, the sensitivity of the OPM was demonstrated by comparing that by a direct weighing method by an analytical microbalance, too. We found the OPM could detect the time-course accumulation of the particles on the filter while the analytical balance was incapable of detecting the difference.

In Chapter 3, the ability in particle concentration measurements was roughly assured for the OPM method. The microscopic methods for determining the particle size distributions are known to be tedious and less precise since the methods are

generally performed manually. To overcome these difficulties, the OPM with the image analysis software and line-sensing mechanism was used in this research. These features could reduce statistical and/or human errors in particle concentration measurements. Indeed, the concentrations obtained by the OPM agreed well with those by an existing direct-reading method, i.e., the light scattering particle counter, indicating the measurement ability by the OPM was comparable to that by the light scattering method (Chapter 3). In addition, the OPM was more advantageous in terms of the particle sizing trueness since it permits direct measurement of the particles and does not rely on measuring the indirect properties such as light scattering. In general, 20 to 30 minutes of the time were required to analyze the particles collected on a filter surface with observed areas of A = 170-420 mm^2 although the required time was dependent on the surface areas observed. The reduction of the time required to analyze sufficient number of the particles could provide opportunities for the precise particle concentration measurements.

The sensitivity of the OPM method, which was clarified in the preceding chapters, can decrease required amounts of the particles for the subsequent gravimetric and/or chemical analyses. Consequently, the decreases of the sampling time and/or rate become possible. The reduction of the sampling time provides opportunities of the time-resolved particle concentration measurements while the decrease of the sampling rates is ultimately attained to the passive sampling methods. The time-resolved measurements of airborne particles are important since the recent works indicate possible association between short-term excursions in fine particle concentrations and adverse health effects. As was described in Chapter 5, the time-resolved measurements of cedar pollens are also strongly desirous in Japan since

the cedar pollinosis patients rather need the concentration information on an hourly basis while the information is presently provided on a daily basis by the local governments. Using a tape filter automatically advanced every set time period, time resolved analyses of airborne particles are possible in future by repeating the measurement cycle of (1) particle sampling, (2) microscopic observation in conjunction with abovementioned chemical and/or biological constituent identification techniques, (3) digital analyses of microscopic images, (4) concentration calculations, and (4) filter exchange.

As was explained in Chapter 6, the passive samplers are essential to accurately characterize the personal exposures to aeroallergens, i.e., coarse allergenic particles. Although it is generally difficult for the passive samplers to collect adequate amounts of the particles for subsequent gravimetric and/or chemical analyses, the OPM is expected to be sufficiently sensitive to quantitate the amounts passively collected. In the last half of this thesis (Chapters 6 and 7), the personal aeroallergen sampler (PAAS), a passive sampler for coarse airborne particles, was introduced as an application of the OPM method. In chapter 6, general features of the PAAS as well as its significance were described. As one of characteristic features of the PAAS, the structure resembling a gimbal was adopted to enable the particle collection surface to be continuously directed upward regardless of inclination of the sampler since the PAAS was designed to collect coarse airborne particles by means of gravitational deposition. Moreover, the PAAS was designed to collect airborne particles right around human breathing area by wearing it around his or her neck. In Chapter 7, the particle collection characteristics of the PAAS were evaluated by the OPM. Specifically, the particle size distributions obtained by the PAAS were compared with those by the IOM

sampler to evaluate particle collection characteristics by the PAAS. The results showed good correlations between the two methods, suggesting usability of the PAAS for long-term personal monitoring of coarse airborne particles including aeroallergens. Unlike existing active samplers, the PAAS is convenient for personal air monitoring because of its simplicity of handling. Therefore, it can be used for a variety of epidemiological studies to investigate relationships between aeroallergen exposures and allergic airway diseases. Using the PAAS in large-scale epidemiological surveys, the detailed mechanisms of allergic airway diseases, which are still uncertain in many aspects, are expected to be elucidated in future.

APPENDIXES

APPENDIX A.
Journal articles published during the Doctoral curriculum

APPENDIX A.1.

N. Yamamoto et al., *J. Aerosol Sci.* 33, 1667 (2002)